

Review

Progress in Modeling of Biomass Fast Pyrolysis: A Review

Pavlo Kostetsky, and Linda J. Broadbelt

Energy Fuels, **Just Accepted Manuscript** • DOI: 10.1021/acs.energyfuels.0c02295 • Publication Date (Web): 11 Sep 2020

Downloaded from pubs.acs.org on September 13, 2020

Just Accepted

"Just Accepted" manuscripts have been peer-reviewed and accepted for publication. They are posted online prior to technical editing, formatting for publication and author proofing. The American Chemical Society provides "Just Accepted" as a service to the research community to expedite the dissemination of scientific material as soon as possible after acceptance. "Just Accepted" manuscripts appear in full in PDF format accompanied by an HTML abstract. "Just Accepted" manuscripts have been fully peer reviewed, but should not be considered the official version of record. They are citable by the Digital Object Identifier (DOI®). "Just Accepted" is an optional service offered to authors. Therefore, the "Just Accepted" Web site may not include all articles that will be published in the journal. After a manuscript is technically edited and formatted, it will be removed from the "Just Accepted" Web site and published as an ASAP article. Note that technical editing may introduce minor changes to the manuscript text and/or graphics which could affect content, and all legal disclaimers and ethical guidelines that apply to the journal pertain. ACS cannot be held responsible for errors or consequences arising from the use of information contained in these "Just Accepted" manuscripts.

1
2
3
4
5
6
7
8
9
10
11
12
13
14
15
16
17
18
19
20
21
22
23
24
25
26
27
28
29
30
31
32
33
34
35
36
37
38
39
40
41
42
43
44
45
46
47
48
49
50
51
52
53
54
55
56
57
58
59
60

Progress in Modeling of Biomass Fast Pyrolysis: A Review

Pavlo Kostetskyy and Linda J. Broadbelt

Department of Chemical and Biological Engineering, Northwestern University, 2145 Sheridan
Rd., Evanston, IL 60208

KEYWORDS: Biomass fast pyrolysis, atomistic modeling, kinetic modeling, machine learning

CORRESPONDING AUTHOR

Prof. Linda J. Broadbelt*

*broadbelt@northwestern.edu

ABSTRACT

Fast pyrolysis of biomass is an important technology in the conversion of lignocellulosic feedstocks to value-added fuels and chemicals. Significant efforts have been dedicated to modeling of these processes to improve the viability of large-scale operation through reactor design, feedstock selection and processing, and optimization of operating conditions, among others. This work is a review of the current progress in the field of modeling of biomass fast pyrolysis processes across multiple length and time scales. Enclosed are summaries of the current state of the art in atomistic and kinetic modeling of biomass fast pyrolysis process toward production of fuels and chemicals. Decomposition of aggregate biomass and its individual components was reviewed for models at various scales, highlighting important considerations. Recent applications of machine learning methods to couple multi-scale phenomena with the goal of reducing computational complexity were also included. Historical context was provided for existing models and correlations, highlighting some of those most widely applied. Some of the shortcomings and bottlenecks in existing models were identified as areas for further study. Finally, potential future directions for the field are suggested with the goal of improving the viability and sustainability of pyrolysis processes and the applications of multi-scale modeling toward this goal.

1 . INTRODUCTION

Thermochemical conversion of plant-derived biomass is an active field of research worldwide, which includes a number of pathways to transform plant biomass into a range of value-added fuels and chemicals, with a long-term vision of ‘drop-in’ applications in retrofitted petroleum refining operations¹⁻⁵. Biomass feedstocks have been classified into three general categories, based on their

origin: first-generation (1G) biomass includes agricultural crops, second-generation (2G) include lignocellulosic biomass such as crop residue and wood, and third-generation (3G) feedstocks include a diverse array of materials such as municipal organic waste and algae^{6, 7}. Biomass is primarily composed of three major components: cellulose, hemicellulose and lignin, with the relative abundance of each fraction varying greatly among different biomass sources (e.g. agricultural residue vs. hardwoods)⁸, with the major molecular constituents of each fraction shown in Figure 1. Cellulose is an ordered linear polymer of glucose units connected by 1,4- β -glycosidic bonds, typically existing in crystalline form, with the function of providing rigid structure to plant cell walls. The role of hemicellulose is to strengthen the structure of the cell wall by interactions with the crystalline cellulose structure. It is an amorphous polymer of different monosaccharides, including D-xylose, D-glucose, D-mannose and others⁹. The structure of lignin is characterized by a complex mixture of phenolic components, referred to as monolignols, that are bonded with ether and carbon-carbon bonds in all dimensions that results in cross-linking and thus a more stable structure relative to the saccharide polymers¹⁰. The function of lignin is to further stabilize and reinforce the structure of sugar polymers in the plant tissues, aid in water transport and aid in preventing bacterial infiltration of plant cells^{11, 12}.

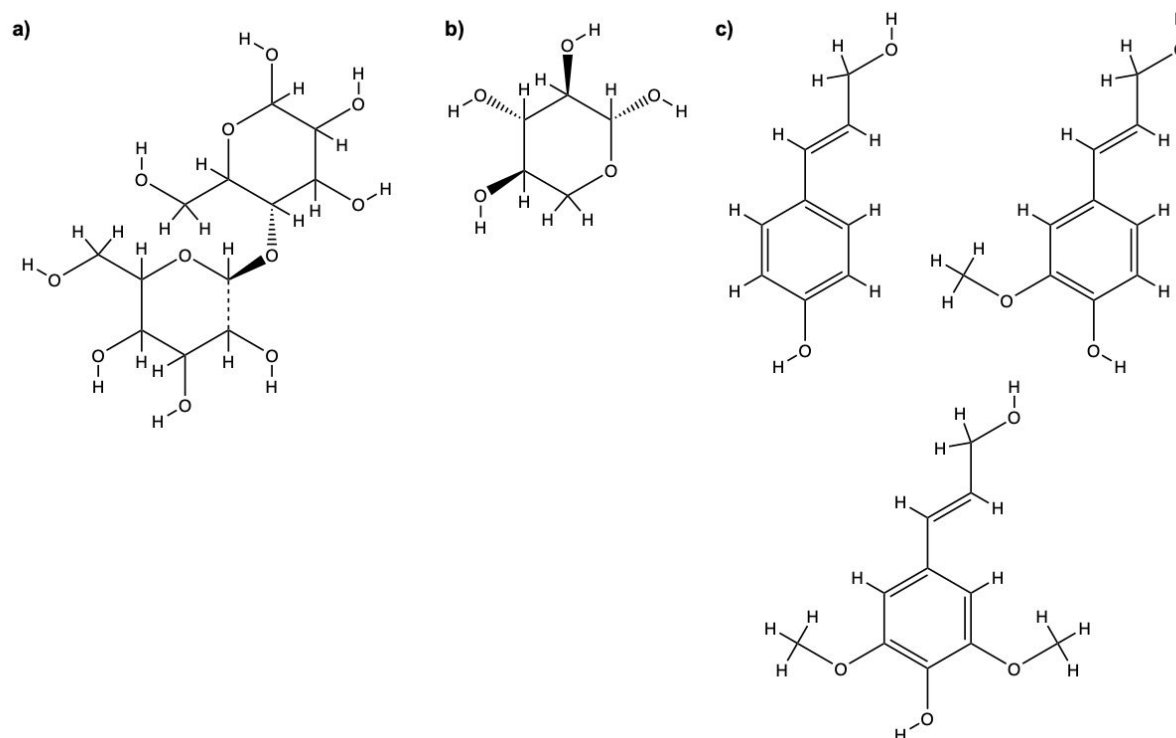


Figure 1. Graphical representation of structural features of the three major fractions of biomass. Namely, a) cellulose, b) hemicellulose and c) lignin are represented by their commonly occurring molecular constituents.

There exist a number of direct and indirect thermochemical pathways to transform biomass feedstocks into value-added products, with three major process categories including gasification, direct liquefaction and indirect liquefaction^{2, 3, 13}. Biochemical transformations are also a key research area in the field of biomass conversion, with significant efforts dedicated over the years. However, these are outside the scope of this review, which focuses on the thermochemical conversion of biomass. Fast pyrolysis of biomass is a thermochemical process in which the feedstock undergoes thermal degradation in the absence of oxygen, which is replaced by an inert or reactive gaseous atmosphere¹⁴. The major products include bio-oil, volatile organics, char and noncondensable gases (NCGs) that form as part of the thermolytic processes within the reactor.

These systems are typically fed by pre-processed biomass that proceeds to react in a heated gaseous atmosphere, rapidly reaching temperatures in excess of 500 °C. The products of such processes can be used directly or further refined toward production of value-added chemicals in catalytic processes^{2-4, 15}. There exist drawbacks to the fast pyrolysis processes, which are directly related to the stoichiometric composition of the biomass itself¹⁶. Specifically, the abundance of oxygen functionalities in the product molecules results in a bio-oil that contains a mixture of decomposition products of highly variable size, polarity, miscibility and stability, with a heating value that is approximately half of conventional crude oil². A number of solutions have been proposed, with most focusing on catalytic deoxygenation¹⁷, leveraging dehydration and hydrodeoxygenation chemistries to synthesize high-value chemicals and fuels. Alternative methods of bio-oil upgrading have been proposed, including non-chemical pathways such as ultrasonic treatment that can promote emulsification of the multiphase mixture and assist with dewatering¹⁸⁻²¹.

Recent work has shown the feasibility of selective production of platform chemicals that are the major products in biomass pyrolysis^{1, 2}. One major source of issues associated with biomass conversion is the inherent heterogeneity of the feedstocks themselves. Different biomass sources have varying composition and hierarchical structure on the cellular, tissue and macro-fraction scale that contain different concentrations of organic and inorganic constituents (Figure 2). The mechanically processed feedstocks vary in size and morphology, playing a key role in the transport of energy, mass and momentum into and out of the reacting particles. In addition, the different solid feedstocks have inherent porosity associated with the requirements of living tissue to transport water and nutrients through the plant body during its lifetime, with the relative fraction and topology of these microstructures varying between the different feedstock sources.

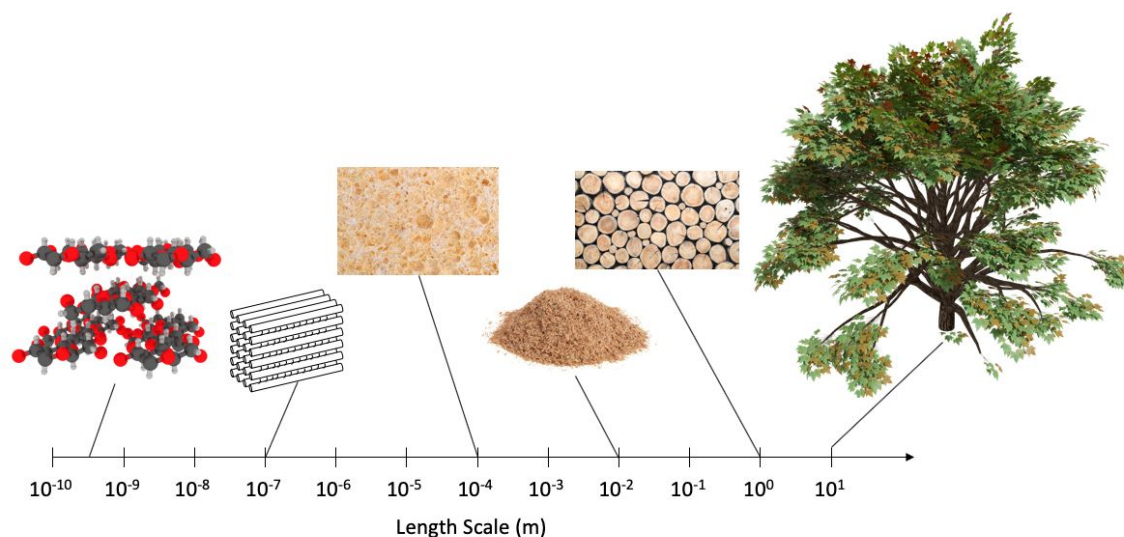


Figure 2. Graphical illustration of the multi-scale nature of lignocellulosic biomass in its application to pyrolysis. From left to right, variability in dimensionality is shown to span from the atomic scale to tissue domains, to macro-scale. Figure snapshots show different representative structures at various length scales – in order from left to right: molecular structure of cellulose, crystalline cellulose fibrils, nutrient-carrying tissue, mechanically-processed biomass, solid wood trunks and living tree.

The successful models of such processes must be able to capture the complex kinetics of chemical reactions in the reactive zone of the reactor, transport of mass and heat into and out of the reacting particles of varying size, and the dynamics of fluid flow through the reactor. Reactor models that include solids, such as sand or catalyst particles, mixed with the biomass must also consider complex fluid dynamics of suspending such mixtures as well as inter-particle interactions. There exist a number of challenges with creating such models, as it is required to couple the different physicochemical phenomena across varying length and time scales. The interconnectedness of reactive and transport phenomena is evident if one considers that reaction rates of biomass particles determine the liquid-phase composition, which in turn changes the

morphology, density and diffusion properties of the individual particles. A systematic framework for development of such models is required, defining the scope, dimensionality, morphology and degree of time dependence (i.e. dynamic vs. steady state)⁷. Differential equations for conservation of mass and energy must be developed, including reaction kinetics of the reacting particles as well as time-resolved changes in size and morphology. Physical properties of all relevant components in the reacting media must be defined, including density, viscosity, conductivity, diffusion coefficients, mass and heat transfer coefficients, and others. Model outputs are typically direct observables such as conversion, concentration, temperature, pressure and particle size/distribution within the reactor⁷. From technoeconomic and process optimization points of view, it is advantageous to minimize the number of processing steps and associated unit operations in biomass conversion processes as part of a greater biorefinery vision toward production of fuels and chemicals^{22, 23}.

Modeling of biomass conversion systems plays a critical role in analysis, development and scale-up of biomass-based technologies. The wide range of physicochemical phenomena occurring at varying time and length scales presents a complex modeling problem, as complex models are typically computationally demanding and require expertise in defining the scope of the model toward maintaining a balance between accuracy and solution time. Predictive computational models of biomass conversion processes can be of great value in development and scale-up by allowing for rapid (*in silico*) screening of system designs, analysis of the effect of operating conditions, improving mass and energy process efficiency, evaluating process modifications, allowing for sensitivity analysis of various process parameters and reducing risks of failure, along with other considerations. Validation with experimental data is important in ensuring flexibility and predictive capacity of computational multi-scale models.

The objective of this review is to give a summary of the recent state-of-the-art in computational modeling of the different aspects of fast pyrolysis of biomass with a focus on coupling of multi-scale phenomena of atomistic and kinetic models of complex reaction networks. Potential areas for further study are suggested toward advancing the current frontier of research in modeling of these systems. Section 2 will include a summary of the multiscale nature of the problem, electronic structure modeling of biomass decomposition and associated kinetic models. Machine learning applications in chemical process modeling will the different biomass fractions decompose be discussed in Section 3, followed by concluding remarks in Section 4. The combination of these overlapping areas of research is important for a deeper understanding of the critical chemical transformations in thermochemical conversion processes toward production of biomass-derived chemicals and fuels.

2 . MECHANISM AND KINETICS

2.1 EXPERIMENTAL AND MODELING COMPLEXITIES

Biomass pyrolysis generates a mixture of hydrocarbon vapors that can be condensed into liquid phase, NCGs, water and char. The relative composition of each of these components in the effluent depends on the nature of biomass particles used, reactor operating conditions and geometry as well as other parameters. Different strategies have been applied to investigate the thermal decomposition of biomass, either focusing on pyrolysis of individual components independently or taking a combinatorial approach of all three pseudocomponents in a single experiment.

The fast pyrolysis mode of operation is characterized by small particle size, decreased residence time (0.5-10 s) and high heating rates (10-200 °C/s) of reacting biomass at increased temperatures of 500-550 °C, resulting in higher bio-oil yields at the expense of solid residues and NCGs. It

should be noted that actual heating rates may vary greatly as a function of biomass source material, particle shape and size, biomass moisture content, local temperature gradients and many others. The parameters that have shown to maximize bio-oil yield are minimizing the residence time of vapor products followed by rapid quenching to form bio-oil, as well as continuous rapid removal of char solids to avoid catalyzing secondary decomposition chemistry. Bio-oil is a general term given to the mixture of condensable pyrolysis products, the properties of which can vary significantly. The stability of this mixture is a concern, as the mixture of hydrophobic and hydrophilic species can phase-separate, continue to react and potentially damage equipment due to its inherent acidity²⁴. A number of experimental and modeling²⁵⁻³⁴ studies have been performed over the years to unravel the complex reaction networks and predict the quantity and composition of pyrolysis effluent³⁵⁻⁴⁰. Recent work has examined different methods of condensing the volatile products via direct and indirect heat exchange, showing increased recovery of heavy ends for direct water-quenched cases⁴¹. However, the scope of this review is limited to the upstream pyrolysis chemistry, making downstream recovery outside the scope of this work.

A number of review papers have summarized the progress in the field of kinetic modeling of solid lignocellulosic biomass pyrolysis over the years. Várhegyi et al. published one of the early reviewed kinetic models of biomass pyrolysis⁴², with a focus on different heating rates, effects of mineral catalysts and sample types such as xylan, lignin and plant biomass samples. Anca-Couce⁴³ reviewed the state-of-the-art models of biomass pyrolysis, including combined models for cellulose, hemicellulose and lignin. In addition, Anca-Couce et al. reviewed kinetic models of biomass pyrolysis, including secondary char formation reactions and effect of the inorganic cations on the observed product distribution⁴⁴. Wang et al.⁴⁵ reviewed a number of macroscopic kinetic modeling methods with comprehensive mechanism schemes, including distributed activation

energy model (DAEM), isoconversional method, detailed lumped kinetic models and kinetic Monte Carlo, to simulate the mass loss behavior of biomass pyrolysis. Dhyani and Bhaskar recently reviewed the current state-of-the-art, focusing on the ideal feedstock, technologies, reactors, and properties of the end product⁴⁶. Zhou et al.⁴⁷ recently reviewed the current state-of-the-art in hemicellulose pyrolysis, focusing on the molecular structure of this polysaccharide, as well as reviewing the status of hemicellulose pyrolysis in terms of experimental investigations, reaction mechanisms and kinetic modeling.

Choi et al. reviewed the most widely used lumped kinetic schemes for the pyrolysis of all three fractions of biomass, with a focus on direct model comparison and validation with experimental results⁴⁸. Mohan et al.⁴⁹ reviewed a number of experimental studies in an effort to gain better understanding of the effect of operating conditions and feedstock type on the observed yields for a wide range of biomass feed types and impurities. Huard et al. have reported recent advances in gas-solid separation technologies, including biomass pyrolysis processes⁵⁰. Yang et al. have reviewed the current state-of-the-art in improving the stability of bio-oil toward storage and transportation applications. These are applied for a range of unit operation applications, including heat exchangers, distillation columns, reactors, fermentors, furnaces, etc. A number of additional review articles with similar scope have been published in recent years, the summary of which becomes redundant, as the authors cover a number of overlapping areas of research, with major contributions from Bridgewater et al.⁵¹⁻⁵⁴, Di Blasi⁵⁵, Butler et al.⁵⁶, Carpenter et al.⁵⁷, Dickerson et al.⁵⁸, Jiang et al.⁵⁹, Sharma et al.⁶⁰, Anca-Couce⁴³, Mostafazadeh et al.⁶¹ and Hameed et al.⁶².

The ability to separate the carbohydrate fractions from the solid biomass and the relatively simple and uniform structure of these polymers has attracted the most research attention over the years for pyrolysis of cellulose and its sugar constituents^{46, 51, 52}. Although this field has been

studied for decades, a number of unanswered questions remain regarding the fundamental elementary mechanisms of product formation in the condensed and gas phase reactions. Some of the key considerations to be addressed in the field have been proposed by Mettler and coworkers⁶³⁻⁶⁵ and include the need to deconvolute the primary and secondary chemistries and address the effect of solvation, char and inorganic salts on the chemistry. In addition, micro-scale phenomena such as heat and mass transfer, aerosol ejection, and the experimental and modeling efforts required to address these were identified as important and currently not sufficiently addressed. The authors proposed a number of potential solutions such as modified reactor configurations and carbohydrate surrogates for cellulose simulations and experiments⁶³ such as cyclodextrin, although its viability as a surrogate has been questioned in recent experimental work⁶⁶.

Capart et al.⁶⁷ performed an experimental study of pyrolysis of microcrystalline cellulose in an inert atmosphere using TGA techniques in isothermal and dynamic heating modes. The authors report experimentally obtained activation energy barriers using a nucleation model to describe the mass loss kinetics. Wang et al.⁶⁸ performed TGA experiments of cellulose pyrolysis with a focus on the catalytic effects of metal salts on the observed product distributions. The authors observed catalytic decomposition of anhydrosugars to small volatile molecules, decreasing the overall yield of levoglucosan by promoting side reactions such as dehydration and decreasing the quality and total yield of desired species. Gao et al.⁶⁹ examined the pyrolysis of cellulose, cellobiose and glucose experimentally, focusing on decomposition at different temperatures, heating rates and residence times. The authors reported on morphology evolution of the reacting particles, relative fractions of bio-oil, char and nonvolatiles, and detailed bio-oil compositions for the pyrolysis of the three carbohydrate types. Burnham et al. have reviewed the current progress on global chemical kinetics of the thermal decomposition of cellulose⁷⁰, showing that the pyrolysis profiles exhibit

1
2
3 sigmoidal character, consistent with one of a sequential, nucleation growth or random-scission
4 global model. Vapor pressure measurements were conducted by Oja et al. for several common
5
6 sugars and have shown that increased temperature regimes not only volatilize the different species,
7
8 but result in secondary reactions, thus making direct measurements difficult⁷¹.
9
10

11
12 Efforts have been focused on characterizing short-lived condensed-phase intermediates, with the
13
14 difficulties stemming from the complexity of the analyte mixtures and lack of resolution with
15
16 conventional analytical instruments. In addition, sample size and mass are known to play a role in
17
18 the evolution of the various products, and a lack of transport limitations in experimental pyrolysis
19
20 studies was confirmed for powder samples of ~500 µg by Zhang et al.⁷² Aerosol ejections were
21
22 characterized by Teixeira et al., using both experimental and computational methods⁷³. Some of
23
24 the major findings included the fact that oligomers of varying size were found in the aerosol
25
26 ejections, with these being the original cellulose components and not formed by repolymerization
27
28 via secondary reactions. For fuel applications, primary pyrolysis products are generally more
29
30 desired, as C-C bond connectivity is maintained, and the ratio of carbon to oxygen is typically
31
32 higher than that of the cellulose feedstock. In addition, these products can be used as feedstocks
33
34 toward production of specific secondary products, generally further increasing the C/O ratio and
35
36 thus the value.
37
38
39
40
41

42 In general, the current state-of-the-art in lignin pyrolysis mechanisms lags behind the work
43
44 performed for sugar components of biomass due to the complexity associated with the highly
45
46 heterogeneous nature of lignin in terms of structure and composition⁷⁴⁻⁷⁶. However, it is generally
47
48 accepted that if the biorefinery approach is to be taken, all of the biomass fractions must be utilized,
49
50 thus necessitating the deeper understanding of these processes and development of accurate and
51
52 robust lignin pyrolysis models. Laskar et al. have examined potential strategies of thermochemical
53
54
55
56
57
58
59
60

conversion of lignin to fuel alternatives⁷⁷. Schutyser et al. recently examined strategies for use of lignin in a biorefinery setting with targeted conversion and upgrading strategies⁴. Biomass feedstocks characterized by high lignin content produce more phenolic compounds, such as syringols, catechols and others⁷⁷. Pyrolysis of lignin results in a complex mixture of oligomers that vary in size and molecular composition¹². The ratio of syringyl (S) and guaiacyl (G) units within the lignin fiber samples has been postulated in the past to control the maximum monomer yield in lignin depolymerization in experimental works of Román-Leshkov and colleagues⁷⁸⁻⁸⁰. However, recent experimental work on lignin depolymerization has shown that additional and/or alternative parameters must be responsible for the observed monomer yields, as the S/G ratio has not been shown to be a predictive parameter⁸¹.

Finally, a number of important studies have examined upgrading of pyrolysis products with the aim of product deoxygenation and selective production of platform chemicals towards production of sustainable chemicals and fuels⁸²⁻⁹⁰. Sharifzadeh et al.⁹¹ studied the kinetics of hydrothermal upgrading of bio-oil, mimicking hydrothermal conditions near the critical point of water by modeling the connectivity of the different types of oxygen functionalities present in the reaction mixture. Detailed analysis of catalytic upgrading is outside the scope of this work and the focus will be maintained on thermal decomposition of biomass.

2.2 ATOMISTIC MODELING OF BIOMASS FAST PYROLYSIS

The development of elementary kinetic models for the pyrolysis of carbohydrates is an active area of research, with increasing degree of complexity over time. Recent advances in experimental methods, improved analytical techniques and advanced computational methods have allowed for detailed elucidation of elementary chemical mechanisms. The use of isotopically-labeled

1
2
3 feedstocks⁹²⁻⁹⁶ and advanced experimental techniques have allowed for identification and isolation
4
5 of key intermediates, thus guiding the development of multi-step kinetic models. Typical
6
7 approaches to computational modeling of carbohydrate pyrolysis energetics involve concurrent
8
9 experiments that identify the major products and assist in narrowing the number of possible
10
11 decomposition pathways that reactants can undergo.
12
13

14
15 Electronic structure calculations have been used to elucidate the potential energy surface (PES)
16
17 of reaction pathways, comprised of sequences of elementary reaction steps toward formation of
18
19 different fragmentation products. Density functional theory (DFT) is a popular choice that can be
20
21 applied to discrete molecular cluster models or periodic representations of the chosen model
22
23 systems, able to quantify the energetics of intermediate ground states and associated transition
24
25 states for any given pathway. Other advanced (higher-accuracy) electronic structure methods have
26
27 also been used to a lesser extent, including Møller–Plesset perturbation theory (MP2-MP4),
28
29 coupled cluster theory (CCSD) and composite methods that perform several calculations toward
30
31 high-accuracy results (CBS-QB3, G4, etc.).
32
33
34

35
36 Advanced computational methods such as ab-initio molecular dynamics (AIMD) can be a
37
38 powerful tool in elucidating preferred pathways for a range of reactions⁹⁷ by sampling low-energy
39
40 states of the PES. Such models are typically computationally-costly but allow for simulation of
41
42 complex systems that include explicit intermolecular interactions with the local chemical
43
44 environment, thus capturing complex interactions that finite clusters cannot. Computational
45
46 efficiency can be increased in cases of low-lying energetic minima by introducing bias for specific
47
48 reaction coordinates in AIMD simulations (referred to as metadynamics⁹⁸), allowing the user to
49
50 sample multiple energy minima on the PES that typically correspond to rare events such as
51
52 elementary steps with high barriers.
53
54
55
56
57
58
59
60

All three fractions comprising biomass have been investigated at varying levels of theory and computational methods, typically using representative model systems of different size and complexity. The following sections focus on thermal decomposition of the three individual fractions of biomass to gain mechanistic insight for each model system. Figures of merit typically include reaction thermodynamics, quantified PES for each pathway, rate-determining steps and corresponding kinetic parameters. Once the energetically preferred steps in the reaction mechanisms have been identified, the calculated kinetic parameters (A and E_a) can be used as input for detailed microkinetic models of chemical reaction networks, comprised of a series of elementary steps. A detailed discussion of kinetic modeling of biomass pyrolysis processes can be found in section 2.4 (*vide infra*).

2.2.1 Cellulose

Cellulose is the most crystalline biomass component, composed of glucose monomers, that has attracted the most research attention in the field biomass pyrolysis. A number of atomistic models have been reported that probe a series of important chemistries, namely depolymerization (glycosidic bond cleavage), ring-opening, carbon backbone fragmentation, dehydration, decarbonylation and others. A summary of elementary step barriers and corresponding reaction energetics obtained from literature discussed in this section are reported in Table 1 (*vide infra*). Values are reported as ranges, as those reported in literature vary significantly with molecular structure and size, computational methods, temperature, etc.

Mayes et al.⁹⁹ reported one of the early computational studies on cellulose depolymerization by reporting DFT-calculated barriers for glycosidic bond cleavage of neat cellulose, concluding that cellulose depolymerization occurs through a concerted mechanism. Using similar methodology, Assary and Curtiss^{100, 101} performed a large number of calculations, probing various decomposition pathways of glucose, cellobiose and fructose, reporting all relevant activation energy barriers and

enthalpies of reaction for all elementary steps. Finally, employing similar cluster model systems, Seshadri and Westmoreland^{102, 103} performed in-depth analysis of the role of proximal hydroxyl groups in facilitating concerted pyrolysis reactions from nearby R-OH spectators such as water. The authors showed that the vast majority of reaction barriers decreased, promoting reactions such as ring-opening, isomerization, pericyclic fragmentation and dehydration for the initial C6 carbohydrates, as well as smaller fragmentation products.

Huang et al.¹⁰⁴ performed DFT calculations on several possible reactions in glucose pyrolysis and did not limit the scope to levoglucosan alone. The four potential pathways resulted in formation of two different C6 anhydrosugars as well as smaller fragmentation products such as glycolaldehyde and acetol. The authors report potential energy landscapes for the four pathways, including kinetic and thermodynamic parameters for a range of temperatures.

Hu et al.¹⁰⁵ performed experimental and computational (DFT) studies of sulfuric acid-catalyzed cellulose pyrolysis, with a focus on chain depolymerization and initial dehydration and ring-opening reactions. Chain effects were approximated by including glycosidic bonds to a capping methyl group meant to represent an additional glucose monomer. The authors show a drastic effect of acid catalysis on the product distribution, favoring products of dehydration reactions. The activation energy barriers and kinetic parameters were reported for uncatalyzed and acid-catalyzed reactions, although it is unclear whether the capping methyl functionalities were sufficiently representative of the presence of another glucose monomer.

Liu et al.¹⁰⁶ probed CO and CO₂ formation pathways with DFT calculations, using two C4 carbohydrates as model reactants. Three potential pathways for each model reactant were proposed, including multiple dehydration, decarbonylation and decarboxylation transition states.

1
2
3 Reaction energetics and associated kinetic parameters were reported for all pathways, including
4
5 temperature effects on reaction thermodynamics along the reaction coordinates.
6

7
8 Hosoya and Sakaki¹⁰⁷ performed DFT and advanced electronic structure calculations (MP4) to
9
10 investigate the energetics of levoglucosan formation from cellulose, with a focus on the role of
11
12 hydrogen bonding interactions between neighboring cellulose molecules. The authors used model
13
14 systems of glucose dimers, and one, two and three-chain oligomers to probe the effect of intra-
15
16 and intermolecular hydrogen bonds on the activation energies toward levoglucosan formation.
17
18 Major findings include the energetically preferred mechanism, activation energies for the
19
20 corresponding elementary steps and comparison with experimental values. It was found that
21
22 increased degree of hydrogen bonding between cellulose chains resulted in increased activation
23
24 energy barriers, with good agreement between the two-chain oligomer models and experimental
25
26 findings.
27
28
29

30
31 Agarwal et al.¹⁰⁸ performed AIMD calculations with metadynamics applied to accelerate the
32
33 frequency of rare events toward sampling the potential energy surface of cellulose fragmentation
34
35 at 327 and 600 °C. The authors identified key reaction steps in forming reactive precursors of
36
37 levoglucosan and HMF in cellulose depolymerization and fragmentation, reporting the
38
39 corresponding energy barriers. The MD tool was shown to be useful in observing key bond
40
41 breaking events in early stages of cellulose fragmentation at two different temperatures, assisted
42
43 by metadynamics for greater computational efficiency. The authors postulated that pre-
44
45 levoglucosan and pre-HMF species are formed in the high-temperature regime, while at low
46
47 temperatures, glucopyranose contracts to glucofuranose, resulting in chain depolymerization and
48
49 formation of the condensed phase.
50
51
52
53
54
55
56
57
58
59
60

1
2
3 Maliekkal et al.¹⁰⁹ recently performed periodic DFT calculations, probing the role of OH groups
4 in stabilizing transition states of glycosidic bond cleavage. The stabilizing role of neighboring
5 sheets of cellulose polymers was postulated to decrease the activation energy, while having a
6 negligible energetic effect on the relative energy of the ground states. This work also included
7 experimental results from the PHASR reactor, which used rapid heating of thin film carbohydrate
8 samples, utilizing a high temperature heat source directly below the sample. Observed yields of
9 levoglucosan were notably lower when compared to single-shot micropyrolyzer experiments
10 performed elsewhere¹¹⁰. It is not clear whether the one-dimensional nature of conductive energy
11 transport to the sample accurately mimics typical pyrolysis conditions and produces representative
12 product composition and yield.
13
14
15
16
17
18
19
20
21
22
23
24
25

26 Finally, it is known that untreated biomass feedstocks contain a range of inorganic salts that can
27 catalyze different chemical reactions and thus affect the product spectrum to a significant degree.
28 Mayes et al.¹¹¹⁻¹¹³ reported on the effect Na^+ ions have on various reaction families relative to the
29 neat carbohydrates, observing a shift in most calculated kinetic parameters, with a general increase
30 in rate constants of most reactions. Several dehydration and ring-opening rate constants were
31 observed to increase by more than an order of magnitude in the presence of the metal ions,
32 providing valuable insight into the effects that inorganic salts may have on individual elementary
33 steps in carbohydrate decomposition.
34
35
36
37
38
39
40
41
42
43
44
45
46
47
48
49
50
51
52
53
54
55
56
57
58
59
60

1
2
3
4
5
6
7
8
9
10
11
12
13
14
15
16
17
18
19
20
21
22
23
24
25
26
27
28
29
30
31
32
33
34
35
36
37
38
39
40
41
42
43
44
45
46
47

Table 1. Reported kinetic parameters and reaction energies for elementary steps involved in cellulose depolymerization and subsequent secondary reactions of glucose-based decomposition products. Values are reported as a range of values from one or several sources, calculated at varying levels of theory, temperature ranges and in presence/absence of mediating species.

Reaction Type	E _a (kJ mol ⁻¹)	ΔE _{rxn} (kJ mol ⁻¹)	Level of Theory	Notes	Reference
Glycosidic cleavage	159 - 254	-149 - 19	G4, MP4(SDQ)/6-311+G(d,p), MP2/6-311+G(d,p), PBE/PWBS, M06-2X/6-311++G(d,p), B3LYP/6-31G(2df,p), B3LYP-D3/6-311G(d,p)	Catalyzed by explicit protic solvents. T = 298 - 773 K	99, 101, 107 - 109
Ring opening	118 - 194	26 - 47	G4, CBS-QB3, uB3LYP/6-311++G(d,p), B3LYP-D3/6-311G(d,p)	Catalyzed by explicit protic solvents. T = 298 K	100, 104, 111 - 113
Dehydration	178 - 372	-28 - 17	G4, CBS-QB3, MP2/6-311++G(3df,3pd), B3LYP/6-31G(2df,p), uB3LYP/aug-cc-pvdz, B3LYP-D3/6-311G(d,p)	Catalyzed by explicit protic solvents. T = 298 - 873 K	100 - 103, 105 - 108, 111 - 113
Pericyclic fragmentation	116 - 166	49 - 51	G4, CBS-QB3	T = 298 K	100, 103, 104
Tautomerization	92 - 272	-39 - -8	G4, CBS-QB3, B3LYP/6-31+G(d,p)	Catalyzed by explicit protic solvents. T = 298 K	100, 104, 111 - 113
Hydride shift	162 - 227	-51 - 61	G4	T = 298 K	100
Decarbonylation	298 - 374	6 - 21	B3LYP/6-31+G(d,p), B3LYP/6-31++G(d,p)	T = 298 K	104, 106
Decarboxylation	273 - 312	-39 - -37	B3LYP/6-31++G(d,p)	T = 298 K	106

2.2.2 Hemicellulose

Hemicellulose polymer chains are more heterogeneous in terms of their constituents and their bonding motifs, resulting in a more amorphous crystal structure, relative to cellulose. Hemicellulose has not attracted as much computational research attention as the cellulose and lignin fractions, although several recent publications have attempted to elucidate the potential energy landscape of pyrolysis reactions, typically employing model compounds to probe the reaction chemistry and propose plausible mechanisms. A summary of elementary step barriers and corresponding reaction energetics obtained from literature discussed in this section are reported in Table 2 (*vide infra*). Values are reported as ranges, as those reported in literature vary significantly with molecular structure and size, computational methods, temperature, etc.

Wang et al.¹¹⁴ focused on the energetics of furfural formation from xylose through computational means, including the effect of solvation via implicit solvation models. The authors proposed a sequence of elementary steps initiated by ring opening via C-O bond cleavage, followed by subsequent hydrogen transfer, dehydration and cyclization reactions toward furfural formation. Implicit solvation was shown to favorably stabilize relevant transition states, suggesting that the presence of water will favorably promote furfural formation.

Huang et al.^{115, 116} have examined the pyrolysis of xylose and xylopyranose via DFT calculations. The authors identified a number of rate-determining steps and reported the associated barriers with typical values near or in excess of 300 kJ/mol. As in the case of glucose and glucose-based carbohydrates, one of the major pathways in xylose pyrolysis involves intramolecular hydrogen transfer and retro-aldol fragmentation chemistry.

Huang et al.¹¹⁷ studied the thermal decomposition of model compounds xylose, O-acetyl xylose and 4-O-MeGlcA in the presence of hydrogen plasma, toward promotion of bond cleavage

1
2
3 reactions. The authors proposed decomposition pathways for several model compounds, including
4
5 both thermal and plasma-mediated chemistries, showing that the presence of hydrogen radicals
6
7 drastically reduces the energy barriers for heterolytic cleavage. The products of carbohydrate
8
9 fragmentation were narrowed to a syngas analogue composed of H₂, CO, CO₂ and C₂H₂.
10
11

12 Wang et al.^{118, 119} also performed DFT calculations on hemicellulose model compounds of xylan,
13
14 arabinose, mannose and galactose. The results included possible decomposition pathways for the
15
16 four model compounds toward formation of furfural, HMF, hydroxyacetone and additional minor
17
18 decomposition products along with the energetic profiles associated with each pathway.
19
20

21 Li et al.¹²⁰ reported a detailed investigation of thermal decomposition of a xylose dimer
22
23 (xylobiose) with DFT calculations, systematically assessing pathway energetics for all
24
25 intermediates. Ring opening and retro-aldol fragmentation were shown to be kinetically dominant,
26
27 while dehydration and decarbonylation were shown to occur in secondary decomposition reactions
28
29 of primary fragmentation products. Furanic products were shown to form through a sequence of
30
31 dehydration and ring contraction reactions of the xylose monomer in its open-chain configuration.
32
33 Hu et al.¹²¹ also report a combined DFT and experimental study on decomposition of hemicellulose
34
35 model compounds xylose, xylobiose and xylan. Their results are in line with those of Li et al.,
36
37 showing that ring opening and glycosidic bond cleavage are key initial steps in a sequence of
38
39 elementary reactions that result in formation of anhydro-D-xylopyranose, furfural, glycolaldehyde,
40
41 formaldehyde and other minor fragmentation products.
42
43
44
45
46

47 Overall, there are many similarities in the low-energy pathways in pyrolysis of cellulose and
48
49 hemicellulose (and their model compounds), including key reaction steps such as glycosidic bond
50
51 cleavage, ring opening/contraction, retro-aldol and Grob fragmentation, isomerization,
52
53 dehydration and decarbonylation. Trends in calculated reaction barriers are typically in line for
54
55
56
57
58
59
60

these reaction families, although the choice of model compound(s) and computational level of theory was shown to affect the calculated values. Furthermore, as hemicellulose is known to form irregular bond networks between monomers, it is not clear whether single monomers or dimers are sufficiently representative of the overall structure. The presence of key functionalities such as hydroxyl and aldehyde groups can promote specific reactions by facilitating hydrogen transfer, glycosidic bond cleavage, and pericyclic fragmentation and dramatically change the PES. As the majority of these studies employed finite molecular clusters of model compounds, it is likely that a significant effect of local chemical environment was not captured, which could lead to erroneous conclusions regarding the rate-determining steps and associated kinetic parameters.

1
2
3
4
5
6
7
8
9
10
11
12
13
14
15
16
17
18
19
20
21
22
23
24
25
26
27
28
29
30
31
32
33
34
35
36
37
38
39
40
41
42
43
44
45
46
47

Table 2. Reported kinetic parameters and reaction energies for elementary steps involved in hemicellulose depolymerization and subsequent secondary reactions of xylose-based decomposition products. Values are reported as a range of values from one or several sources, calculated at varying levels of theory, temperature ranges and in presence/absence of mediating species.

Reaction Type	E _a (kJ mol ⁻¹)	ΔE _{rxn} (kJ mol ⁻¹)	Level of Theory		Notes	Reference
Glycosidic bond cleavage	214 - 352	64 - 328	M06-2X/6-31+G(d,p), B3LYP-D3/6-311G(d,p)		T = 298	120, 121
Ring opening	147 - 204	-10 - 61	M06-2X/6-31++G(d,p), M06-2X/6-31+G(d,p), B3LYP-D3/6-311G(d,p), B3LYP/6-31++G(d,p), B3LYP/6-31G(d,p), B3LYP/6-31++G(d,p)		Catalyzed by explicit protic solvents. T = 298 - 1100 K	114, 115 ^a , 116, 117, 118, 120, 121
Dehydration	217 - 365	-16 - 69	M06-2X/6-31++G(d,p), M06-2X/6-31+G(d,p), B3LYP-D3/6-311G(d,p), B3LYP/6-31++G(d,p), B3LYP/6-31G(d,p), B3LYP/6-31++G(d,p)		Catalyzed by explicit protic solvents. T = 298 - 1100 K	114, 115 ^a , 116, 117, 118, 120, 121
Pericyclic fragmentation	120 - 361	-38 - 103	M06-2X/6-31++G(d,p), M06-2X/6-31+G(d,p), B3LYP-D3/6-311G(d,p), B3LYP/6-31G(d,p)		T = 298 - 1100 K	115 ^a , 117, 118, 120, 121
Tautomerization	82 - 299	-13 - 61	M06-2X/6-31++G(d,p), M06-2X/6-31+G(d,p), B3LYP-D3/6-311G(d,p), B3LYP/6-31++G(d,p), B3LYP/6-31G(d,p)		Catalyzed by explicit protic solvents. T = 298 - 1100 K	114, 115 ^a , 116, 117, 118, 120, 121
Decarbonylation	159 - 335	-168 - -5	M06-2X/6-31++G(d,p), M06-2X/6-31+G(d,p), B3LYP-D3/6-311G(d,p) B3LYP/6-31+G(d,p), B3LYP/6-31G(d,p)		T = 298 - 1100 K	115 ^a , 116, 117, 118, 120, 121
Decarboxylation	333 - 294	-56 - -49	B3LYP/6-31G(d,p), B3LYP/6-31++G(d,p)	B3LYP/6-31G(d,p),	T = 298	117, 118

^aValues reported at 298 K

2.2.3 Lignin

The composition and morphology of lignin are significantly more heterogeneous than cellulose and hemicellulose, forming a bond network between its constituent monomers in different directions and resulting in highly-amorphous structures. The pyrolysis chemistry of such feedstocks is difficult to deconvolute due to a large number of potential fragmentation products in initial cleavage reactions leading to formation of large oligomers with a high degree of heterogeneity in their reactive moieties. Much of the computational studies have employed relatively simple model compounds such as monomers and dimers of basic constituents.

There exist a number of potential intermediates of varying size and composition in lignin pyrolysate, characterized by intact or partially-reacted aromatic rings substituted with hydroxy and methoxy groups, such as guaiacol, syringol, catechol, coniferyl, sinapyl, and p-coumaryl, among others. The complex mixtures can undergo subsequent secondary reactions, resulting in a complex network of elementary steps and a series of unimolecular and bimolecular reactions that may involve concerted, heterolytic and homolytic chemistries¹²²⁻¹²⁴. A number of computational studies on pyrolysis of model lignin compounds have been carried out. The potential energy landscapes (PES) of the various competing reaction pathways may be of use as input in construction of kinetic models based on these model compounds.

A summary of ranges of elementary step barriers and corresponding reaction energetics obtained from literature discussed in this section are reported in Table 3 (*vide infra*). Values are reported as ranges, as those reported in literature vary significantly with molecular structure and size, computational methods, temperature, etc. It should be noted that as the number of different model compounds and possible homolytic pathways is far greater in lignin pyrolysis, this summary will be limited to heterolytic chemistry and associated elementary steps. The reader is encouraged to

more closely examine the literature of interest, where detailed bond dissociation energies and PESs for the homolytic pathways can be tracked for the relevant species.

Li et al.¹²⁵ screened a range of pyrolytic lignin species, including model compounds, using several experimental techniques such as HPLC/Qtof-MS, GPC and 2D HSQC NMR, in combination with DFT calculations. A number of species were classified according to their physical properties, identifying potential candidates for production of high value products as well as potential coke precursors from pyrolytic lignin. Advanced electronic structure calculations were performed by da Silva and Bozzelli¹²⁶ to quantify the detailed potential energy surface of thermal decomposition of o-quinone methide, an intermediate in pyrolysis of lignin and its model compounds. The authors reported calculated kinetic parameters as a function of temperature for the rate-determining steps and compared these to experimental values, with a difference of 4.1 kcal/mol.

Asatryan et al.¹²⁷ examined the potential energy surface of p-coumaryl alcohol (p-CMA) reactivity assisted by OH radicals via DFT calculations. The authors found a number of low-energy dehydration reactions that generated a range of O- and C-centered intermediate radicals, found to form phenolic compounds during pyrolysis experiments. Jiang et al. examined the effect of alkali metal chlorides on the reaction energetics of 1-methoxy-2-(4-methoxyphenethoxy) benzene, a dimer molecule used as a model compound, with DFT calculations. The authors proposed dimer decomposition pathways in the presence of inorganic salts via C_β-O homolytic and concerted cleavage, based on the calculated PES. Shaw and Zhang¹²⁸ used DFT calculations to assess the thermal stabilities and bond dissociation enthalpies for 27 common phenolic compounds found in bio-oil. Main findings included the relative bond strengths of various molecular fragments bound

1
2
3 to the phenol ring, in part rationalizing low thermal stabilities of methoxy phenol compounds such
4
5 as guaiacol and syringol.
6

7
8 Cao et al.¹²⁹ investigated potential pretreatment methods for lignocellulosic biomass such as
9
10 low-temperature plasma to promote bond dissociation in corn- and poplar-derived lignin samples
11
12 with experimental and computational methods. β -O-4 aryl ether was used as a model compound
13
14 in assessing several decomposition pathways, with the ether bond dissociation shown to be the
15
16 preferred initial reaction that is also promoted by the presence of plasma. Chen et al.¹³⁰ further
17
18 examined the pyrolysis mechanisms of β -O-4 lignin model dimer with experimental and DFT
19
20 methods. The authors proposed a set of mechanisms that are dominant at different temperatures,
21
22 with the homolytic reactions dominating at low temperatures and concerted reactions followed by
23
24 secondary decomposition prevalent at elevated temperatures.
25
26

27
28 Hu et al.¹³¹ investigated the potential energy surface of vanillin structural conformers with
29
30 electronic structure calculations, including bond dissociation energies of the various substituents
31
32 on the aromatic ring. The BDEs are useful in assessing the bonds that would be preferentially
33
34 cleaved during pyrolysis of complex reactant mixtures. Wang et al. also performed DFT
35
36 calculations to assess the energetics of unimolecular and bimolecular decomposition pathways of
37
38 vanillin. They proposed initial reaction steps for vanillin decomposition, benzene formation
39
40 pathways and intermolecular hydrogen abstraction energetics. Analogously, Liu et al.¹³²⁻¹³⁵ and
41
42 Huang et al.¹³⁶ proposed decomposition pathways for model compounds such as guaiacol and 4-
43
44 benzyloxyphenol, and the dissociation of α -O-4 bonded dimers via experimental and
45
46 computational means. Also, using the same methodology, Jiang et al.¹³⁷ analyzed the initial
47
48 decomposition products of 1,2-bis(3,5-dimethoxyphenyl)propane-1,3-diol, probing several
49
50 competing pathways for initial decomposition of the reactant molecule. The authors proposed a
51
52
53
54
55
56
57
58
59
60

number of homolytic and concerted decomposition pathways from the parent carbohydrate, providing detailed potential energy surfaces and BDEs for each pathway. An identical methodology was employed by Jiang et al.¹³⁸ to examine intermolecular hydrogen abstraction reactions by radicals formed during primary pyrolytic reactions. The authors proposed a reaction network in which radicals are stabilized by hydrogen donors such as primary pyrolysis products and lignin polymers.

Yunker and coworkers¹³⁹⁻¹⁴¹ have performed extensive electronic structure calculations with methods at multiple levels of theory to assess the energetics for thermal decomposition of multiple model compounds such as β -5 arylcoumaran, o-OH-anisole, o-OH-phenoxy radical and phenethyl phenyl ether. They reported relevant BDEs and energetic landscapes for homolytic decomposition chemistries of these model compounds. Competing pathways were assessed for C-O and C-C bond cleavage, identifying the energetically-preferred mechanisms, including a comparison in method accuracy between DFT and advanced electronic structure methods (CCSD(T)). In addition, the effect of varying ring substituents on the model compounds was assessed and reported.

Parthasarathi et al.¹⁴² performed extensive DFT calculations examining thermal decomposition energetics of 65 lignin model compounds, probing the effects of different bonding configurations that connect arene rings for a range of model species. The authors assembled a set of BDEs for C-C and ether cleavage reactions, showing a preference for ether bond cleavage in most cases. A strong correlation between C-C bond distance and BDE was reported, with longer bonds resulting in more favorable bond cleavage. Sheng et al.¹⁴³ used experiments and DFT calculations to examine the dominant reaction mechanisms in pyrolysis of 2-phenethyl phenyl ether trimers, tetramers and synthetic polymers containing β -O-4 linkages. Radicals as product species were not observed experimentally, suggesting that radical chemistry is not likely to occur, relative to

1
2
3 hemolytic and concerted scission reactions. Furutani et al.¹⁴⁴ and Altarawneh et al.^{145, 146} performed
4
5 extensive electronic structure calculations for thermal decomposition of model compounds such
6
7 as guaiacol and catechol. The authors examined different fragmentation mechanisms, providing
8
9 energetic landscapes for the proposed mechanism.
10
11
12
13
14
15
16
17
18
19
20
21
22
23
24
25
26
27
28
29
30
31
32
33
34
35
36
37
38
39
40
41
42
43
44
45
46
47
48
49
50
51
52
53
54
55
56
57
58
59
60

1
2
3
4
5
6
7
8
9
10
11
12
13
14
15
16
17
18
19
20
21
22
23
24
25
26
27
28
29
30
31
32
33
34
35
36
37
38
39
40
41
42
43
44
45
46
47

Table 3. Reported kinetic parameters and reaction energies for elementary steps involved in primary and secondary reactions of lignin model compounds. Values are reported as a range from one or several sources, calculated at varying levels of theory and temperature ranges.

Reaction Type		E _a (kJ mol ⁻¹)	ΔE _{rxn} (kJ mol ⁻¹)	Level of Theory	Notes	Reference
C-O cleavage	bond	187-264	-149 - 61.2	M06-2X/6-311++G(d,p), M06-2X/6-31+G(d,p), B3LYP/6-31G(d,p), B3LYP/6-31G(d)	T = 298K	123 - 125, 129, 130, 143
C-C cleavage	bond	210 - 423	-2 - 61	B3LYP/6-311+G(d,p)	T = 298K	134, 137
Dehydration		323 - 411	-85 - 411	CBS-QB3, B3LYP/6-311G(2d,d,p), B3LYP/6-311+G(d,p)	T = 298K	122, 137, 145
Isomerization		244 - 321	-134 - 364	CBS-QB3, B3LYP/6-311G(2d,d,p), B3LYP/6-311+G(d,p)	T = 298K	122, 130, 145
Dehydrogenation		334 - 454	181 - 206	CBS-QB3, B3LYP/6-311++G(d,p), B3LYP/6-311+G(d,p)	T = 298K	135, 144, 145
Decarbonylation		133 - 368	23 - 130	CBS-QB3, B3LYP/6-311++G(d,p), B3LYP/6-311+G(d,p)	T = 298K	135, 144, 145

Recent work by Dellon et al.¹⁴⁷ identified and compiled a library of chemical structures, toward characterization of the complex lignin thermolysis product mixtures, including the various model compounds summarized in this section.

In summary, the current state of the art in computational modeling of thermal decomposition of the three biomass fractions and their model compounds remains in its early stages for a number of reasons. The majority of studies employ finite cluster models of model compounds which does not account for intermolecular interactions in the reactive region, although it is well known that neighboring molecules can facilitate various reactions through favorable arrangements that facilitate bond-breaking events. Tools such as periodic DFT can capture such interactions by sampling the PES through ab-initio molecular dynamics. Often, the methodology employed such as choice of level of theory and basis set size are not uniform and as a result, direct comparison of results is difficult. Nevertheless, a significant body of work has already been assembled, and the accumulated data such as BDEs, conformer energies, and PESs can be assembled into libraries toward informing data-driven approaches such as machine learning algorithms.

2.3 MECHANISTIC MODELING

Pyrolysis of biomass can occur over a range of temperatures, with the product distributions varying significantly with temperature. The process of biomass pyrolysis is initiated by evaporation and degradation of water and extractable species from the biomass particles, typically below 200 °C. Hemicellulose and cellulose decompose in the temperature ranges of 200-300 °C and 300-400 °C, respectively, with the variability in these temperature ranges being primarily a function of particle size and biomass feedstock type. The complex structure of lignin and its variability result in a wide range of decomposition temperatures (200-900 °C), with continuous

1
2
3 degradation at varying rates observed over the full range of temperatures¹⁴⁸. Kinetic models of
4 biomass pyrolysis require understanding of thermal degradation of the different components as
5 well as the interaction of these at reaction conditions.
6
7

8
9
10 In general, biomass pyrolysis reactions can be classified as primary and secondary^{74, 75, 149-151},
11 with the distinction of consequence being the relative position in the sequence of reactions.
12 Although detailed biomass pyrolysis mechanisms have not been fully elucidated, it is known that
13 primary reactions involve depolymerization of the different biopolymers. The major products from
14 the different biomass fractions vary significantly, but it is generally understood that the monomers
15 do not undergo significant decomposition in the primary phase. Secondary reactions involve
16 decomposition of the primary products that are either catalyzed or thermally driven and involve
17 the formation of low molecular weight products of varying size and functionalities.
18
19

20
21
22 It is known that primary pyrolysis products in bio-oil from cellulose and hemicellulose fractions
23 include anhydrosugars, such as levoglucosan, that are produced by cleavage of glycosidic bonds
24 in the cellulose polymer chains and comprise the majority of bio-oil^{152, 153}. In addition, smaller
25 decomposition products of varying size and functionality (furans, pyrans, acids, aldehydes,
26 ketones, etc.) also comprise the liquid effluent, the composition of which can vary significantly
27 even at identical operating conditions, simply by varying the biomass feedstock or reactor
28 configuration^{110, 154, 155}. Glycolaldehyde, glyoxal, acetol, pyruvaldehyde and other C2-C4 products
29 are produced in increased quantities in the presence of inorganic salts in the biomass feed, which
30 is attributed to fragmentation of glucose and anhydrosugars. Patwardhan et al.¹⁵⁶ and Dalluge et
31 al.¹⁵⁷ performed an experimental study of fast pyrolysis of hemicellulose, reporting the product
32 distribution for purified feedstock and accounting for the presence of inorganic salts. The authors
33 reported a greater yield of sugars and light oxygenates in the treated samples relative to the
34
35
36
37
38
39
40
41
42
43
44
45
46
47
48
49
50
51
52
53
54
55
56
57
58
59
60

1
2
3 untreated. Primary lignin pyrolysis products can repolymerize into secondary products that can be
4 thermally stable and result in decreased yields of desired products and char formation, with recent
5 work reporting several promising strategies of mitigating such chemistry¹⁵⁸.
6
7

8
9
10 Lin et al.¹⁵⁹ have proposed an indirect furan formation mechanism via a levoglucosan (LGA)
11 intermediate which is formed from cellulose depolymerization and dehydration reactions. It should
12 be noted that the dominant pathway is still unknown and remains debated in literature. Pyrans are
13 a subgroup of six-member ring products of cellulose decomposition that are typically formed by
14 water elimination reactions such as those at the ¹C and ⁴C carbons toward complex pyran
15 formation¹⁶⁰. The knowledge base of pyran formation mechanisms relative to furans remains an
16 underexplored area of research, with no dominant pathway proposed. Milosavljevic et al. have
17 looked at secondary reactions in cellulose pyrolysis and have shown that the heating rates of
18 biomass samples strongly affect the volatilization of products^{152, 153}.
19
20
21
22
23
24
25
26
27
28
29
30

31 Modeling of biomass fast pyrolysis processes requires understanding of the structure and
32 composition of the feedstocks, spanning different length scales from cellular to tissue domains of
33 plants. The relative fractions of the major components vary between different feedstocks, generally
34 consisting of 50% cellulose, 20–30% hemicellulose and 20–30% lignin. In addition, minor
35 fractions of complex carbohydrates such as resins and fatty acids, along with inorganic salts (Na⁺,
36 K⁺, Ca²⁺, Mg²⁺, Cl⁻, etc.), exist as part of the biomass^{24, 43, 51, 52}. The catalytic effect of inorganic
37 salts present in the biomass samples on pyrolysate composition has been examined by a number
38 of authors, including Wang⁶⁸, Raveendran et al.¹⁶¹, Wang et al.¹⁶², Trendewicz et al.¹⁶³ and others.
39 Inorganic cations such as K⁺ and Na⁺ promote dehydration chemistry, significantly increasing
40 observed char yields and small fragmentation products at the expense of bio-oil.
41
42
43
44
45
46
47
48
49
50
51
52
53
54
55
56
57
58
59
60

At fast pyrolysis operating conditions, thermal reactions of cellulose, hemicellulose and lignin can be coupled at elevated temperatures, resulting in interactions that favor formation of light condensable products from cellulose as well as inhibiting char formation from lignin compounds. The vast majority of kinetic models developed to date have examined the independent decomposition of the three biomass components, as is described in the following section.

2.4 KINETICS OF BIOMASS PYROLYSIS

The focus of much of the research on development of global kinetic models implemented different experimental methodologies such as thermogravimetric analysis (TGA), calorimetry, fast pyrolysis and hybrid systems, varying process parameters such as temperature, heating rate, sample size, feed type and a number of others^{148, 164}. Typical experiments monitor one or several properties of interest as a function of changing thermal environment around the reacting particles. In addition, different analytical techniques can be applied to identify and quantify the thermal decomposition products within some error tolerance. Techniques such as TGA have been a widely applied experimental method to analyze biomass fragmentation by tracking the mass change as a function of time for a given sample. The change in sample mass is monitored and used as a measure of the extent of thermal degradation. Debate persists in the community whether it is a valid technique due to large variability in the experimental conditions, such as heating rates, between experiments. Typically, TGA experiments have been conducted in a non-isothermal operating regime in which the reactor temperature is ramped at a constant rate, typically on the order of several degrees per second, until a temperature set point is reached or observable reactions become negligible. TGA experiments can also be conducted in an isothermal operating regime, in which the biomass samples experience a constant reaction temperature for the duration of the experiment.

One of the major drawbacks to isothermal operation is the presence of temperature gradients and the inability to account for initial sample heating, devolatilization and fragmentation reactions, in addition to requiring multiple experiments for each specific temperature regime.

Although TGA has been widely used in obtaining mass-loss data as input for kinetic model development for a number of different feedstocks and heating rates, disagreements remain regarding the viability of these methods to accurately capture the intrinsic kinetics of decomposition. Specifically, selection of heating rates and biomass samples has been shown to significantly affect the pyrolysis kinetics, and therefore makes direct comparison of different results difficult.

Several key process features characterize fast pyrolysis, including rapid heating rates into pre-processed, fine biomass particles at temperatures of ca. 500 °C at short residence time of pyrolysis vapors and aerosols that are quenched rapidly downstream to maximize the yield of liquid products^{47, 51, 52, 165}. A number of parallel and sequential reactions occur during fast pyrolysis of biomass, including depolymerization, dehydration, ring opening/closing, isomerization, Grob fragmentation, retro-aldol fragmentation, decarboxylation, decarbonylation, char formation and others^{47, 110, 155}. A complete understanding of the reactions occurring in the reactive zone and the complex interplay between kinetics and transport phenomena would be critical when attempting to design and scale up pyrolysis systems. The kinetics of biomass pyrolysis are typically modeled with explicit mechanistic or simplified empirical models.

Empirical models are most often based on observations, utilizing some degree of parameter fitting to experimental data that were collected for a range of conditions. The predictive nature of such models is limited, and the end-use cases for empirical models are typically for the set of conditions at which the experimental observations were made. Furthermore, the experimental data

collected for fitting of such models should be representative of full-scale operating conditions, which can be difficult for the complete lifetime of the reacting particles due to variability in the residence time for different reactor configurations¹⁴⁹. Alternately, mechanistic models are characterized by fundamental representation of the system and are based on multiple components such as elementary steps to capture the feature space to a greater extent (relative to empirical models) and have some predictive capacity. The majority of the kinetic formulations used to describe solid biomass decomposition make use of Arrhenius-type equations (Equation 1) to produce a reaction network of interconnected elementary steps.

$$k(T) = A \times \exp\left(-\frac{E_a}{RT}\right) \quad (1)$$

These formulations estimate the rate constant $k(T)$ by combining the pre-exponential (frequency) factor (A) that reflects entropic changes at the transition state and the activation energy barrier (E_a) that needs to be overcome to achieve the product state. The product of these two terms is an estimate of the frequency of reaction events occurring for specific reactant(s). The exponential term, containing the activation energy (E_a), is to a much greater degree a function of temperature relative to the frequency factor.

Thermal analysis is a set of experimental methods to extract information about the kinetics of biomass decomposition under different thermal conditions¹⁶⁶. These can be conducted in an isothermal regime, in which multiple experiments are performed at different temperatures, with the reacting samples experiencing a set temperature for the duration of the experiment. Alternately, differential heating techniques have also been used extensively, in which the reacting samples experience a range of temperatures in a single experiment by controlling the rate of heating of the sample. The mass of the sample can be monitored during the experiment, utilizing microbalances with a pre-set heating rate of the plate surface.

Both approaches have inherent advantages and drawbacks, and debate remains regarding the usefulness and applicability of each. For example, isothermal techniques typically require multiple experiments to sample a wide enough range of temperatures, resulting in extensive expenditure of time and effort. In addition, there remains a transient heat-up period that biomass samples experience for each temperature point, possibly introducing transport artifacts to the kinetic data. Differential heating methods can have difficulty with reproducibility, as both the temperature and heating rates are known to affect decomposition kinetics. The accuracy and reliability of these methods can be improved by performing multiple experiments at different heating rates. In addition, several kinetic studies on interactions between the three fractions and their effect on product distributions for a wide range of conditions have been performed – no clear conclusions could be drawn, largely due to the complexity of these systems and limitations of analytical equipment¹⁶⁷⁻¹⁷¹.

Researchers have implemented the isoconversional technique, keeping the rate of reactant conversion ($d\alpha/dt$) constant, thus allowing the rate of reaction to be a function of concentration and temperature¹⁶⁶.

$$\frac{d\alpha}{dt} = k(T) \times f(\alpha) = A \times \exp\left(-\frac{E_a}{RT}\right) \times f(\alpha) \quad (2)$$

Where $f(\alpha)$ is a function of reactant concentration, which can be rewritten as:

$$\ln\left[\frac{d\alpha}{dt}\right] = \ln[A \times f(\alpha)] - \frac{E_a}{RT} \quad (3)$$

A ‘lumped’ activation energy (E_a) term can be obtained from isoconversional experimental data by plotting the rate of change of conversion vs. $1/T$, assuming no transport limitations¹⁷².

A major assumption in these kinetic models is that the Arrhenius expression is applicable in solid-state reactions of biomass, although this has been disputed by a number of authors¹⁷³⁻¹⁷⁵. In

fact, the extensive variability in kinetic parameters for biomass thermal decomposition has been attributed to the non-applicability of classical Arrhenius expressions to solid-state reactions¹⁷⁵. Although conflicts remain regarding the applicability of such mathematical expressions, no universal alternative that would generalize temperature dependence of complex processes has been proposed. An important assumption made is the absence of transport limitations in the reacting samples, which is incorrect in many cases, as it is known that temperature and concentration gradients exist in reacting samples¹⁷³⁻¹⁷⁵, thus making it critical to carefully select the experimental conditions that will reflect intrinsic reaction kinetics. A comprehensive listing of models describing solid-state reactions has been in circulation for nearly four decades and reports commonly used mathematical expressions in modeling of biomass pyrolysis, as shown in Table 4.

Table 4. Mathematical forms of expressions used in modeling of pyrolysis phenomena in solid-state reactions¹⁶⁶.

Reaction Model	$f(\alpha) = \left(\frac{1}{k}\right)\left(\frac{d\alpha}{dt}\right)$	$g(\alpha) = kt$
Reaction Order		
Zero Order	$(1 - \alpha)^n$	α
First Order	$(1 - \alpha)^n$	$-\ln (1 - \alpha)$
n th order	$(1 - \alpha)^n$	$(n - 1)^{-1}(1 - \alpha)^{(1 - n)}$
Nucleation		
Power Law	$n(\alpha)^{(1 - 1/n)}; n = 2/3, 1, 2, 3, 4$	$\alpha^n; n = 3/2, 1, 1/2, 1/3, 1/4$
Exponential Law	$\ln (\alpha)$	α
Avrami-Erofeev	$n(1 - \alpha)[\ln (1 - \alpha)]^{(1 - 1/n)}; n = 1, 2, 3, 4$	$[-\ln (1 - \alpha)]^{1/n}; n = 1, 2, 3, 4$
Prout-Tompkins	$\alpha(1 - \alpha)$	$\ln [\alpha(1 - \alpha)^{-1}] + C$
Diffusion		

1-D	$1/2\alpha$	α^2
2-D	$[-\ln(1-\alpha)]^{-1}$	$(1-\alpha)\ln(1-\alpha) + \alpha$
3-D (Jander)	$3/2(1-\alpha)^{2/3}[1-(1-\alpha)^{1/3}]^{-1}$	$[1-(1-\alpha)^{1/3}]^2$
3-D (Ginstling-Brounshtein)	$3/2[(1-\alpha)^{-1/3} - 1]^{-1}$	$1 - 2/3\alpha - (1-\alpha)^{2/3}$
Contracting Geometry		
Contracting Area	$(1-\alpha)^{(1-1/n); n=2}$	$1 - (1-\alpha)^{1/n}; n=2$
Contracting Volume	$(1-\alpha)^{(1-1/n); n=3}$	$1 - (1-\alpha)^{1/n}; n=3$

A number of different models have been proposed to predict the kinetics of biomass pyrolysis that vary in complexity as reflected by their mathematical formulation. The experimental data produced by TGA experiments have been used for model development, predicting the evolution of NCGs, condensable vapors and char. The simplest of the kinetic models have approximated the complex physicochemical phenomena of pyrolysis reactions as irreversible single-step mechanisms in which the three major components are produced based on lumped kinetic parameters. These models have significant limitations in their ability to predict product distributions, as they rely on kinetic parameters that lump a large number of chemical reactions and possibly mass transfer phenomena^{24, 51, 166}. Kinetic network models have been developed by several different groups, including academic and commercial sources: Niksa¹⁷⁶ and Solomon et al.^{177, 178} have developed coal devolatilization models based on several phenomena that govern the decomposition of coal based on breakdown of the macro structure of coal along with simultaneous evolution of volatile species.

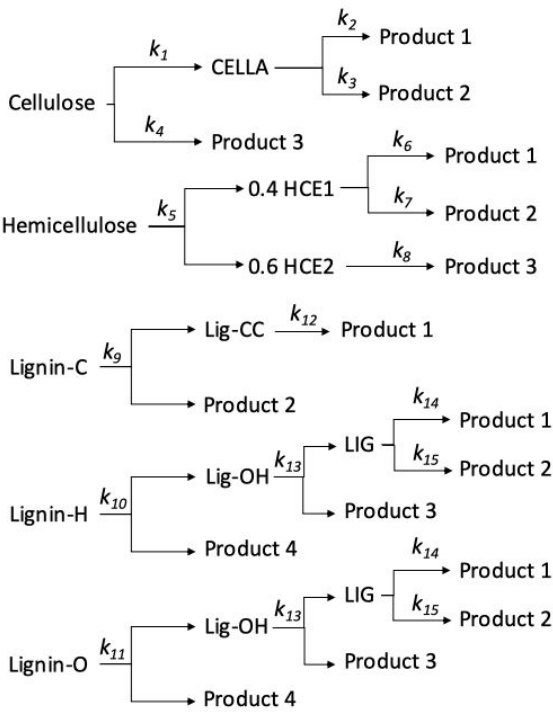
Several models have been developed for the thermal decomposition of all three fractions of biomass, taking the form of predicting the evolution of the major product fractions via lumped kinetic parameters. TGA data were used for development of the lumped kinetic models of varying complexity by a number of authors over previous decades. Shafizadeh and Chin developed one of

the earliest models for wood decomposition, including three competitive reactions toward formation of NCGs, tar and char¹⁷⁹. One of the most commonly applied models in biomass pyrolysis is that of Broido and Shafizadeh, which is a single-step model in which NCGs tar and char fractions are formed directly and secondary chemistry is not considered. The formation of the product fractions was modeled to proceed through activated intermediates of cellulose, hemicellulose and lignin^{179, 180}. An identical framework was used by Miler and Bellan towards modeling of the mass evolution in pyrolysis of the three major fractions, with modified stoichiometric coefficients, corresponding to the three major product fractions¹⁸¹.

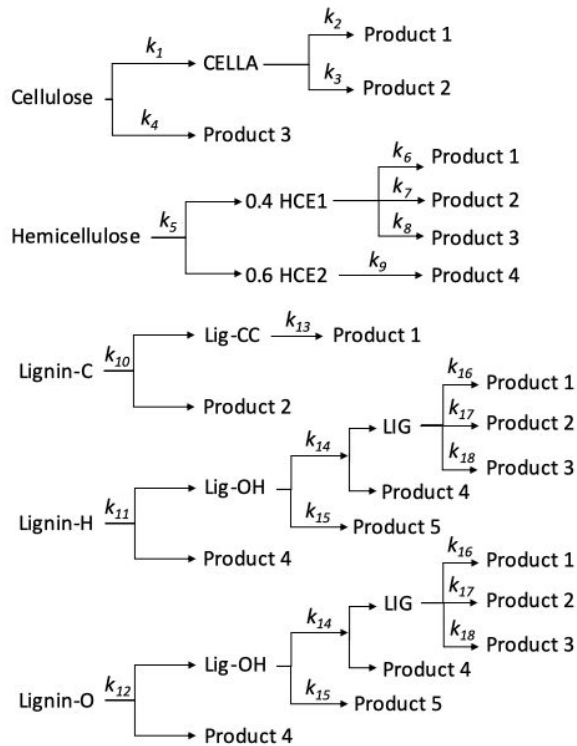
Di Blasi extended the Broido-Shafizadeh mechanism to include secondary tar cracking reactions, resulting in further formation of NCGs and char¹⁸². Corbetta et al. recently developed a multi-step mechanism for pyrolysis of multi-component biomass, resulting in production of multiple explicit products ranging from levoglucosan to NCGs¹⁸³. The authors refined the lignin pyrolysis model by characterizing it as a combination of three reference components with different degrees of methoxylation: LIG-H, LIG-O and LIG-C, which contain higher molar fractions of hydrogen, oxygen and carbon, respectively. Enumerated product placeholders represent multiple products with varying stoichiometric coefficients that correspond to experimentally observed species yields. Ranzi et al. have also proposed a kinetic model based on the three biomass components that was very similar to that of Corbetta et al. with different stoichiometric coefficients and kinetic parameters that were also developed by fitting to experimental results^{184, 185}. Finally, the kinetic framework developed by Ranzi and Corbetta was modified by Blondeau et al.¹⁸⁶ for high heating rates, more typical of fast pyrolysis, by adjusting the relevant stoichiometric coefficients and kinetic parameters. The model also included heat transport. A graphical summary of all of the aforementioned mechanisms is shown in Table 5.

Table 5. Summary of combined kinetic models for the three biomass fractions

Graphical Representation of Kinetic Model	Reference
$\text{Biomass} \begin{cases} \xrightarrow{k_1} \text{NCG} \\ \xrightarrow{k_2} \text{Tar} \\ \xrightarrow{k_3} \text{Char} \end{cases}$	Shafizadeh et al. (1976) ¹⁷⁹
$\begin{aligned} \text{Cellulose} &\xrightarrow{k_{1,\text{cellulose}}} \text{Active Cellulose} \\ \text{Active Cellulose} &\begin{cases} \xrightarrow{k_{2,\text{cellulose}}} X_{\text{cell}}\text{Char} + (1-X_{\text{cell}}) \text{NCG 1} \\ \xrightarrow{k_{3,\text{cellulose}}} \text{Tar} \xrightarrow{k_4} \text{NCG 2} \end{cases} \end{aligned}$	Broido & Shafizadeh (1975) ¹⁸⁰
$\begin{aligned} \text{Hemicellulose} &\xrightarrow{k_{1,\text{hemicell}}} \text{Active Hemicellulose} \\ \text{Active Hemicellulose} &\begin{cases} \xrightarrow{k_{2,\text{hemicell}}} X_{\text{hemicell}}\text{Char} + (1-X_{\text{hemicell}}) \text{NCG 1} \\ \xrightarrow{k_{3,\text{hemicell}}} \text{Tar} \xrightarrow{k_4} \text{NCG 2} \end{cases} \end{aligned}$	Mller & Bellan (1997) ¹⁸¹
$\begin{aligned} \text{Lignin} &\xrightarrow{k_{1,\text{lignin}}} \text{Active Lignin} \\ \text{Active Lignin} &\begin{cases} \xrightarrow{k_{2,\text{lignin}}} X_{\text{cell}}\text{Char} + (1-X_{\text{cell}}) \text{NCG 1} \\ \xrightarrow{k_{3,\text{lignin}}} \text{Tar} \xrightarrow{k_4} \text{NCG 2} \end{cases} \end{aligned}$	
$\text{Biomass} \begin{cases} \xrightarrow{k_1} \text{NCG} \\ \xrightarrow{k_2} \text{Tar} \\ \xrightarrow{k_3} \text{Char} \end{cases} \quad \text{Tar} \begin{cases} \xrightarrow{k_4} \text{NCG 2} \\ \xrightarrow{k_5} \text{Char 2} \end{cases}$	Di Blasi (1996) ¹⁸²



Ranzi et al.
(2008)^{184, 185}



Corbetta et al.
(2013)¹⁸³

Gomez et al. have studied devolatilization kinetics of treated and untreated wood samples applying a summative model for thermal degradation of the three pseudocomponents¹⁸⁷. Hu et al. also examined biomass pyrolysis kinetics of the three major fractions for several biomass types by applying normal distribution functions to include ranges of activation energies for all three components¹⁸⁸.

Heating rates have long been known to affect the yield and composition of bio-oil obtained as pyrolysis products. Generally, it is known that high heating rates at elevated temperatures produce higher yields of liquid products and low yield of char, whereas low heating rates and low temperature regimes result in extensive char formation. It is interesting to note that the char residue formed at low heating rates tends to retain the macroscopic structure of the biomass feed. Recent work has examined the reaction chemistry of levoglucosan, which has been shown to repolymerize into anhydro-oligosaccharides at low heating rates (~ 3 K/s), whereas pure levoglucosan simply evaporates at typical fast pyrolysis conditions (~ 200 K/s), suggesting that repolymerization of anhydrosugars occurs on a significantly longer time scale relative to volatilization. Additionally, oligosaccharides of varying degree of polymerization (DP 2-7) have been observed by modulation of heating rates, leveraging radiative heating towards rapid quenching¹⁸⁹⁻¹⁹¹. Additional studies into oligosaccharide formation were recently performed by Liu et al.¹⁹² and Gong et al.¹⁹³.

Global kinetic schemes have been popular due to their relative simplicity and limitations of most analytical equipment to track the evolution of individual products during experiments. Further complexity has been added to the original global models by adding multiple parallel reactions occurring at the same time, enabling more predictive power in estimating the fractions of char, condensable and NCGs. In the case of cellulose pyrolysis, the formation of an important intermediate liquid phase of “active cellulose” was incorporated into the global kinetic schemes,

proposed to form by weakly endothermic “melting” of the crystalline solid. One of the main limitations of these models, however, remains the lack of predictive capacity at vastly different operating conditions and variability in the feedstock.

The lack of predictive capacity was further addressed by addition of multiple consecutive reactions into the global schemes, thus allowing for a more detailed mechanistic picture. The drawback to addition of sequential chemical reactions in the pyrolysis schemes lies in the potential for error propagation through the reaction chains, potentially amplifying small discrepancies in initial reaction steps toward the subsequent steps. In addition, as the characterization of short-lived intermediates in the condensate is generally not feasible, most of the intermediate steps in the sequential chains are in the end based on assumptions informed by the end products observed. Distributed activation energy models applied originally to estimate the distribution of volatile products in coal pyrolysis have found application in biomass pyrolysis¹⁹⁴. The basis of these models is the representation of a range of activation energies as a continuous distribution (such as Gaussian) to reflect the great heterogeneity in bond dissociation activation energies of the various fragmentation products in pyrolysis processes¹⁹⁵⁻¹⁹⁹.

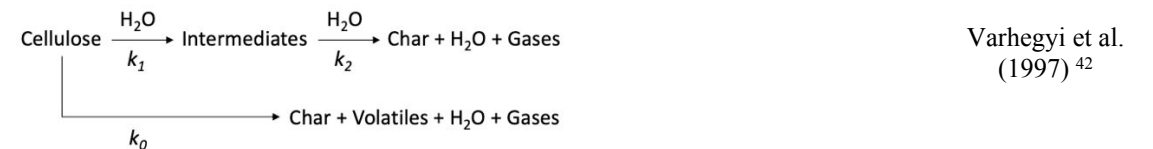
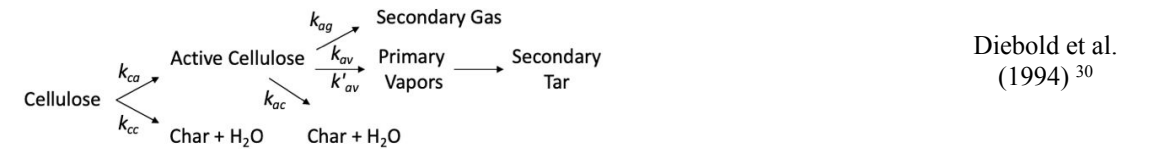
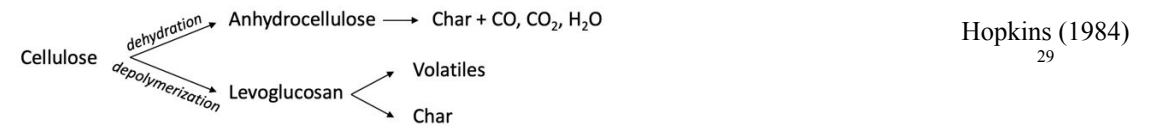
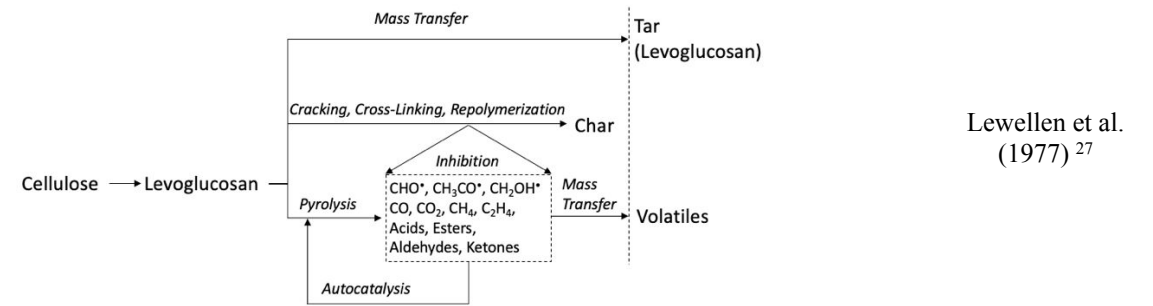
Cellulose has been the most widely studied component of biomass, with some of the more popular kinetic models developed in the last several decades reported in Table 6. The evolution of kinetic models has resulted in formulations of increasing complexity, including increasing numbers of intermediate products, which go on to react further toward the final products. The majority of formulations for modeling the kinetics of cellulose pyrolysis have also been based on lumped kinetic models that do not explicitly account for individual chemical species, with the Broido–Shafizadeh^{26, 28} model being one of the earliest and most widely used. These reaction schemes have been updated over the years by including additional complexity, thus enabling the

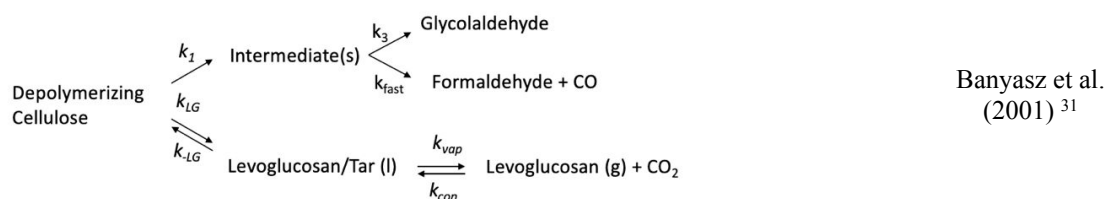
prediction of individual components of the pyrolysis products³¹. The kinetics of cellulose pyrolysis have been represented with irreversible lumped kinetic parameters capturing the global reaction chemistry, resulting in a number of early kinetic schemes developed by a number of authors^{26-31, 42, 200}. Burra et al. recently applied kinetic models with multiple sequential steps in pyrolysis of different feedstocks, using TGA-DSC experiments, with the number of intermediate steps chosen manually as a function of feedstock type²⁰¹.

Recent work of Vinu et al.²⁰² and Zhou et al.^{110, 155} has accounted for a large number of competing and sequential reactions with multiple intermediate products in the pyrolysis of glucose and glucose-based carbohydrates. In addition, more recent work by Zhou et al.²⁰³ applied a similar methodology to develop a detailed kinetic model of hemicellulose pyrolysis. The authors have combined experimental and computational methods (e.g. atomistic modeling) to develop detailed kinetic models that accounted explicitly for the formation of individual product species as well as chain depolymerization of parent sugar chains. Fragmentation of biomass polymers was modeled explicitly, accounting for depolymerization kinetics of cellulose and hemicellulose through the method of moments. Good agreement with experimental results over a range of conditions was observed for all models.

Table 6. Graphical summary of lumped kinetic models of cellulose pyrolysis in chronological order. This summary is meant to be representative and is by no means an exhaustive listing of all models proposed in the given time period.

Graphical Representation of Kinetic Model	Reference
---	-----------





3. ADVANCES IN MACHINE LEARNING AND APPLICATIONS TO PYROLYSIS MODELING

3.1 COMMONLY USED METHODS

Machine learning has found a number of applications in the fields of chemical engineering, including molecular modeling and simulation^{204, 205} and materials discovery and design^{206, 207}, with supervised learning methods finding the most applications to date. Recent efforts have been made to leverage machine learning (ML) techniques to reduce the computational requirements in modeling various aspects of these processes without sacrificing accuracy or flexibility as reported by Ali et al.²⁰⁸ Neural Networks (NN), Genetic Programming (GP), Fuzzy Logic (FL), Support Vector Machines (SVM), Response Surface Methodology (RSM) and other types of ML methods have been useful in process modeling and classification, provided that large data sets are available for training and validation²⁰⁸.

Artificial neural networks (ANN) have seen a sharp rise in applications toward reducing the computational cost of modeling complex physicochemical phenomena over the last two decades^{205, 209-212} and have been some of the most popular of the different ML methods. ANNs were developed to mimic the function of neuron clusters in the human brain, consisting of a large number of processor nodes or neurons arranged into multiple layers. The input and output layers are

composed of discrete nodes that are visible to the user and correspond to independent variables and dependent output, respectively. One or more hidden layers can exist between the input and output layers, these being responsible for applying a series of functions to the input data, with the specific functions varying between the different types of neural network applied. The connections between neurons in the different layers are weighted to prioritize the signals being passed, with the numerical values of the weighting factors being allowed to change as the neural network is trained on data sets in an iterative manner, until the output signal achieves the desired value. The total number of hidden nodes varies between studies, as it is a function of the type of NN applied, type of system examined and the size of the training data set. No general methodology exists to determine the number of hidden nodes, and the determination of these is typically done manually until the desired degree of accuracy is achieved. Ali et al.²⁰⁸ have summarized several types of ANN that have found applicability in chemical process systems, as outlined in Table 7.

Table 7. Comparison of some major ANN structures applicable in modeling of chemical systems, along with their key features, advantages and limitations, as reported by Ali et al.²⁰⁸

Type of ANN	Key Features	Advantages	Limitations
Feed forward neural networks (FFN)	Fixed function and require large amount of training data	Accurately approximate continuous functions	Slow convergence
		Easy to implement	Lack dynamics
			Mainly used for static function approximation
Internally recurrent net (IRN)	Characterized by time-delayed feedback connections from output of hidden nodes back to inputs of hidden nodes	Capable of estimating process with changing variable dynamics	Difficult to initialize
		No limit for the number of states	Training can be time-consuming

Externally recurrent net (ERN)	Contain time-delayed feedback connections from output layer to a hidden layer	Easy to initialize	Number of states must be the same as model outputs
		Simple design and can use current values to initialize states	Training can be time consuming
Radial basis function neural networks (RBFNN)	Basis function used can be Gaussian or wavelets	Less sensitive to sensor noise	Most suitable for classification problem
		Faster training	Large number of hidden nodes needed
Recurrent trainable neural network (RTNN)	Hidden layer is the recurrent layer and the other two layers are based on back propagation	Faster convergence	Not versatile
		Less complexity in the design	Slow training due to sequential structure
Shape-tunable neural network (MNN)	Allow tuning of weight between neurons and saturation function of each neurons simultaneously	Sensitive to plant changes but still provide good estimation even with varied parameters	Greatly depends on sampling time and initial parameters

Thermal decomposition chemistry involves a large number of chemical transformations in highly correlated systems with complex interplay between chemical kinetics and transport of heat and mass. Furthermore, the evolution of reacting particles results in structural change of the particles, potentially changing the kinetic behavior due to additional catalytic promotion. One of the main issues with the application of ANNs to kinetic modeling is the poor generalization of these models if the topology of reaction networks is to be ignored. Many publications that apply ANNs have treated the relationships between input and output variables as a “black box,” thus contributing to the difficulties of generalizing the applicability of these models. Furthermore, to achieve sufficient accuracy, large data sets are required to train the networks and verify their performance as applied to a separate data set used for validation. Parameter selection is another important consideration that can greatly impact the performance of the model and its applicability.

3.2 RECENT ADVANCES

Hough et al.^{213, 214} have applied machine learning methods, namely ANNs to address the issue of solution time for chemical reaction networks of large size. Computationally prohibitive models of detailed chemical reaction networks can be addressed with machine learning tools by training the ANNs on appropriate data sets and applied towards prediction of kinetic parameters. Such approaches can decrease the required computational resources and make possible the coupling of time-resolved kinetics and transport phenomena within the reacting particles. Furutani et al.²¹⁵ recently applied the kinetic model proposed by Hough et al. to predict the product composition for pyrolysis of three different types of lignin, differentiated by the type of pre-treatment with which lignin was produced. Good agreement with experimental findings was observed for the production of the major products, capturing the experimental trends for the three different lignins.

Hua et al.²¹⁶ examined the use of convolutional neural networks (CNN) in modeling of large-scale naphtha pyrolysis kinetics. The authors applied graph theory to represent a total of 4694 reactions involving 142 species in the naphtha pyrolysis network. The relevant features of the pyrolysis reactions were identified and extracted via network characterization in which structural motifs of the network graph were identified and used to represent the reactants in the network. The authors show good predictive ability of the model to estimate the product yields of various hydrocarbons in the pyrolysis effluent. Similar approaches can be taken for explicit modeling of the different fractions of biomass, alleviating the lack of detail typical in lumped kinetic models.

Lerkkasemsan et al. have recently applied adaptive neuro-fuzzy inference systems (ANFIS) toward the modeling of pyrolysis kinetics of reed canary grass and solid wood²¹⁷. The model was a combination of ANNs and the fuzzy inference system with the ability to learn from the available data set, applying a hybrid learning algorithm that utilizes a steepest descent method and a least squares estimator. The model generates a set of human-readable linguistic rules toward the input

parameters, with reaction temperature and duration being used as the input. The output results were the conversion and mass yields of the major product fractions, with significantly better model performance relative to the commonly applied Arrhenius-type models for a range of experimental conditions.

Nieto et al. have recently used ML methods towards prediction of fuel heating values (HHV) in biomass torrefaction studies²¹⁸, using fundamental properties of the feedstock such as elemental composition, reaction temperature and time to estimate the HHV of crop residue biomass. A hybrid algorithm based on support vector machines (SVM) combined with a simulated annealing (SA) optimization technique was developed and applied. The algorithm was able to prioritize and rank the most significant physicochemical properties of the materials and estimate HHVs that agreed well with experimental results. The use of such models would reduce the need for costly experimental analysis due to large heterogeneity in the type of feedstock.

Jiang et al. have looked at the preparation of straw-derived activated carbon via catalytic pyrolysis methods, applying regression, support vector regression and random forest regression as predictive models²¹⁹. Zhu et al. have utilized deep learning methods in reactor monitoring for pyrolysis applications²²⁰. Their deep learning approach can be used to assist operators by providing detailed real-time information of the reactor, using thermal imaging of the reactor as input data.

Francisco-Fernandez et al. have used a number of ML methods, including Linear Discrimination Analysis (LDA), Logistic Regression, Naïve Bayes Classification (NBC), k Nearest Neighbors (k -NN), Support Vector Machines (SVM) and Neural Networks (NN), to classify different types of woody biomass, using TGA data as input.²²¹ The first, second and third derivatives of the thermogravimetric curves were used as model inputs, quantifying the rate of mass decrease as a function of temperature. The authors showed that differential TGA data can be used as valid input

for classifying different types of woody biomass, with good classification probabilities for all methods employed. Noise reduction via local polynomial smoothing of the experimental curves significantly improved the likelihood of correct classification.

Nabavi et al. applied NN methods to model a methanol to olefin (MTO) reactor and to predict main product yields as a function of reactor temperature, water/methanol ratios in the feed, and reactor space-time²²². Maran et al. have applied response surface methodology (RSM) and ANNs towards modeling and optimization of biodiesel production from different vegetable oils, assisted by ultrasound agitation of the reactive mixtures^{19, 21}. System descriptors such as reaction temperature, reaction time, catalyst concentration and the alcohol-to-oil ratio were used as input data, with the conversion of fatty acid methyl esters (FAME) being the output parameters. The authors showed that an ANN with the topology of 4-7-1 (seven neurons in the hidden layer) was significantly more effective in predicting FAME conversion relative to RSM. The authors showed that catalyst concentration was the process variable with the greatest effect on the observed conversion values. Stamenkovic et al. have studied the optimization of base-catalyzed ethanolysis of vegetable oils toward biofuel production by utilizing RSM and ANNs²²³. Cheng et al. have utilized Genetic Algorithm-based Evolutionary Support Vector Machine (GA-ESVM) toward prediction of physicochemical properties of biodiesel in a recent study²²⁴.

Saldana et al. have used SVM methods to predict the properties of fuel mixtures as a function of molecular structure of component molecules and their relative concentration in the fuel mixture²²⁵. The authors were able to predict flash points for a range of fuel mixtures by using as input the thermodynamic properties of individual components, namely the vapor pressure and activity coefficients, referred to as Le Chatelier rule-based models. SVM methods were shown to perform poorly, relative to the Le Chatelier rule-based models. The extension of such methodology can be

1
2
3 useful in predicting vapor-liquid equilibrium data for complex mixtures of pyrolysis products in
4
5 catalytic and non-catalytic applications. Arabloo and coworkers have utilized SVM methods to
6
7 optimize the operating conditions for coal gasification processes, showing good agreement with
8
9 experimental observations²²⁶.
10
11

12 13 14 4 . FUTURE RESEARCH DIRECTIONS 15 16

17 18 4.1 MODEL ACCURACY AND COMPLEXITY 19 20

21 The field of biomass fast pyrolysis is currently in the early stages of commercialization at scale,
22
23 as some significant issues remain that must be addressed by the community – some of them
24
25 discussed in this review. Issues with the scale of operation, feedstock variability and pretreatment,
26
27 bio-oil quality and upgrading, downstream product use, and a number of others remain as a
28
29 roadblock to widespread use. Modeling of these processes can be useful in accelerating the design
30
31 and optimization of such systems, spanning different length and time scales. However, even the
32
33 most elaborate and detailed models confront limitations in their predictive capacity, and it is
34
35 important to clearly define the scope of such models, as well as validate the models with
36
37 experimental data. Nevertheless, a number of companies across the globe have succeeded in design
38
39 and operation of non-agricultural biomass conversion processes toward fuel and chemicals
40
41 production at a scale as large as multiple million gallons per year of bio-oil production. Companies
42
43 such as Ensyn Inc., BTG Inc., Anellotech Inc., Fortum Inc., Genting Inc. and others were early
44
45 developers and implementors of biomass conversion technology with a focus on fuels production.
46
47
48
49

50 The wealth of experience in the petrochemical and coal^{226, 227} industries can be useful in
51
52 accelerating the process of making pyrolysis technology viable – at scale. For example, catalytic
53
54 processes have long been used in petroleum refining operations, with standardized procedures
55
56
57
58
59
60

existing for catalyst screening, system design, model development and validation. Models are refined and validated experimentally, with careful considerations of scale-up, feed composition, catalyst formulation and long-term loss of activity, among others. Accurate models of biomass fast pyrolysis and downstream catalytic upgrading are critical for design of the complete systems, as well as being useful input for additional modeling such as technoeconomic analysis²²⁸ and environmental impact via life cycle analysis. These models are an important component of the overall design process, as the economic viability and net carbon balance are vital to widespread acceptance from the commercial and public stakeholders. As the pyrolysis and secondary upgrading units are critical components of biomass conversion processes, accurate and robust models (validated by experimental data) for a range of feedstocks, reactor geometries and operating conditions are vital.

Utilizing ML approaches toward kinetic model reduction while explicitly accounting for individual product components, can be a powerful tool in decreasing the computational cost of large reaction networks as shown by Hough et al.^{213, 214} This is important as the majority of the existing kinetic models utilize lumped kinetic parameters that vary significantly for different feedstock types and operating conditions, thus limiting their predictive capacity to a narrow range of conditions at which the parameters were obtained.

4.2 LONG-TERM TRENDS AND MODELING OF BIOMASS PYROLYSIS

Broadly speaking, the proposed schemes for the biorefinery model have underutilized the inherent value of the different biomass fractions, by *a priori* prioritization toward the production of fuels²²⁹. For example, cellulose is the most abundant and least structurally complex component of biomass with good crystallinity, capable of being separated from parent biomass by a number

of well-established methods. It is currently envisioned as a precursor for fuel production via a number of government initiatives, although it is plausible that cellulose can be used in production of higher-value products, leveraging the ordered structure of cellulose, as compared to hemicellulose or lignin. This approach may be of value in the current economic climate, as the energy markets remain volatile and dominated by low-cost alternatives such as shale gas and liquid petroleum. The economic viability of biomass conversion processes remains tenuous with current market trends, and high-value products such as specialty chemicals can be essential in the near-term.

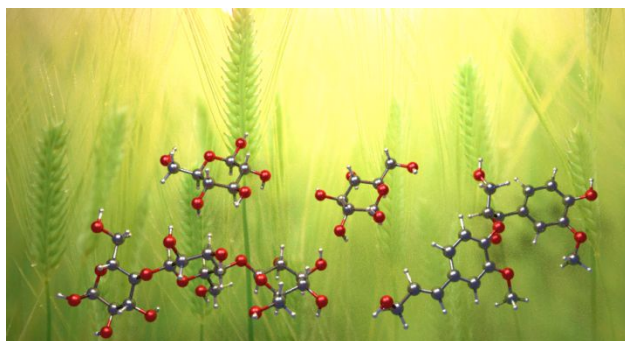
Long-term trends in the field of fuels and chemicals appear to be moving in the direction of further integration of industrial processes with cyber-based systems and advanced manufacturing technologies for data collection, process monitoring, control and optimization²³⁰⁻²³². The integration of such processes can improve operational efficiency, reduce operating cost and generate greater total value for society as a whole. Detailed microkinetic models of the chemical transformations in biomass pyrolysis processes can provide valuable insight into the dominant primary and secondary chemical reactions, toward maximizing the production of desired products in the effluent. ML techniques are a significant component of these processes and can be used to reduce the computational complexities and enable modeling of complex systems. Further research into model reduction through ML-based methods and implementation in multi-scale models at the particle or reactor scales would be a valuable addition to the field as a whole. Generally-speaking, one of the roadblocks to extending the application of ML methods is availability, processing and storage of large data sets that are typically required for training and validation of ML-based models.

1
2
3
4
5
6
7
8
9
10
11
12
13
14
15
16
17
18
19
20
21
22
23
24
25
26
27
28
29
30
31
32
33
34
35
36
37
38
39
40
41
42
43
44
45
46
47
48
49
50
51
52
53
54
55
56
57
58
59
60

ACKNOWLEDGEMENTS

The authors are grateful for financial support from the National Science Foundation (CBET-1435228 and CBET-1926412).

For Table of Contents Only



References:

1. Huber, G. W.; Corma, A., Synergies between bio- and oil refineries for the production of fuels from biomass. *Angewandte Chemie-International Edition* **2007**, 46, (38), 7184-7201.
2. Kunkes, E. L.; Simonetti, D. A.; West, R. M.; Serrano-Ruiz, J. C.; Gartner, C. A.; Dumesic, J. A., Catalytic conversion of biomass to monofunctional hydrocarbons and targeted liquid-fuel classes. *Science* **2008**, 322, (5900), 417-421.
3. Alonso, D. M.; Bond, J. Q.; Dumesic, J. A., Catalytic conversion of biomass to biofuels. *Green Chemistry* **2010**, 12, (9), 1493-1513.
4. Schutyser, W.; Renders, T.; Van den Bosch, S.; Koelewijn, S. F.; Beckham, G. T.; Sels, B. F., Chemicals from lignin: an interplay of lignocellulose fractionation, depolymerisation, and upgrading. *Chemical Society Reviews* **2018**, 47, (3), 852-908.
5. Huber, G. W.; Iborra, S.; Corma, A., Synthesis of transportation fuels from biomass: Chemistry, catalysts, and engineering. *Chemical Reviews* **2006**, 106, (9), 4044-4098.
6. Yang, C.; Li, R.; Zhang, B.; Qiu, Q.; Wang, B.; Yang, H.; Ding, Y.; Wang, C., Pyrolysis of microalgae: A critical review. *Fuel Processing Technology* **2019**, 186, 53-72.
7. Sharifzadeh, M.; Sadeqzadeh, M.; Guo, M.; Borhani, T. N.; Konda, N. V. S. N. M.; Garcia, M. C.; Wang, L.; Hallett, J.; Shah, N., The multi-scale challenges of biomass fast pyrolysis and bio-oil upgrading: Review of the state of art and future research directions. *Progress in Energy and Combustion Science* **2019**, 71, 1-80.

8. Sluiter, A.; Hames, B.; Ruiz, R.; Scarlata, C.; Sluiter, J.; Templeton, D.; Crocker, D., Determination of Structural Carbohydrates and Lignin in Biomass. *US National Renewable Energy Laboratory, Golden, Colorado, NREL/TP-510-42618* **2008**.
9. Zhang, J.; Choi, Y. S.; Yoo, C. G.; Kim, T. H.; Brown, R. C.; Shanks, B. H., Cellulose-Hemicellulose and Cellulose-Lignin Interactions during Fast Pyrolysis. *ACS Sustainable Chemistry & Engineering* **2015**, 3, (2), 293-301.
10. Ragauskas, A. J.; Williams, C. K.; Davison, B. H.; Britovsek, G.; Cairney, J.; Eckert, C. A.; Frederick, W. J.; Hallett, J. P.; Leak, D. J.; Liotta, C. L.; Mielenz, J. R.; Murphy, R.; Templer, R.; Tschaplinski, T., The path forward for biofuels and biomaterials. *Science* **2006**, 311, (5760), 484-489.
11. Ragauskas, A. J.; Beckham, G. T.; Biddy, M. J.; Chandra, R.; Chen, F.; Davis, M. F.; Davison, B. H.; Dixon, R. A.; Gilna, P.; Keller, M.; Langan, P.; Naskar, A. K.; Saddler, J. N.; Tschaplinski, T. J.; Tuskan, G. A.; Wyman, C. E., Lignin Valorization: Improving Lignin Processing in the Biorefinery. *Science* **2014**, 344, (6185), 709.
12. Rinaldi, R.; Jastrzebski, R.; Clough, M. T.; Ralph, J.; Kennema, M.; Bruijninx, P. C. A.; Weckhuysen, B. M., Paving the Way for Lignin Valorisation: Recent Advances in Bioengineering, Biorefining and Catalysis. *Angewandte Chemie-International Edition* **2016**, 55, (29), 8164-8215.
13. Mirkouei, A.; Haapala, K. R.; Sessions, J.; Murthy, G. S., A mixed biomass-based energy supply chain for enhancing economic and environmental sustainability benefits: A multi-criteria decision making framework. *Applied Energy* **2017**, 206, 1088-1101.

14. Zhang, H. Y.; Xiao, R.; Wang, D. H.; He, G. Y.; Shao, S. S.; Zhang, J. B.; Zhong, Z. P., Biomass fast pyrolysis in a fluidized bed reactor under N₂, CO₂, CO, CH₄ and H₂ atmospheres. *Bioresource Technology* **2011**, 102, (5), 4258-4264.
15. Eagan, N. M.; Kumbhalkar, M. D.; Buchanan, J. S.; Dumesic, J. A.; Huber, G. W., Chemistries and processes for the conversion of ethanol into middle-distillate fuels. *Nature Reviews Chemistry* **2019**, 3, (4), 223-249.
16. Neves, D.; Thunman, H.; Matos, A.; Tarelho, L.; Gomez-Barea, A., Characterization and prediction of biomass pyrolysis products. *Progress in Energy and Combustion Science* **2011**, 37, (5), 611-630.
17. Gamlie, D. P.; Wilcox, L.; Valla, J. A., The Effects of Catalyst Properties on the Conversion of Biomass via Catalytic Fast Hydropyrolysis. *Energy & Fuels* **2017**, 31, (1), 679-687.
18. Li, Y. P.; Wang, T. J.; Liang, W.; Wu, C. Z.; Ma, L. L.; Zhang, Q.; Zhang, X. H.; Jiang, T., Ultrasonic Preparation of Emulsions Derived from Aqueous Bio-oil Fraction and Diesel and Combustion Characteristics in Diesel Generator. *Energy & Fuels* **2010**, 24, (3), 1987-1995.
19. Maran, J. P.; Priya, B., Modeling of ultrasound assisted intensification of biodiesel production from neem (*Azadirachta indica*) oil using response surface methodology and artificial neural network. *Fuel* **2015**, 143, 262-267.
20. Yi, M. X.; Huang, J.; Wang, L. F., Research on Crude Oil Demulsification Using the Combined Method of Ultrasound and Chemical Demulsifier. *Journal of Chemistry* **2017**, Article ID 9147926.

21. Maran, J. P.; Priya, B., Comparison of response surface methodology and artificial neural network approach towards efficient ultrasound-assisted biodiesel production from muskmelon oil. *Ultrasonics Sonochemistry* **2015**, 23, 192-200.
22. Demirbas, M. F., Biorefineries for biofuel upgrading: A critical review. *Applied Energy* **2009**, 86, S151-S161.
23. Demirbas, A., Competitive liquid biofuels from biomass. *Applied Energy* **2011**, 88, (1), 17-28.
24. Bridgwater, A. V.; Meier, D.; Radlein, D., An overview of fast pyrolysis of biomass. *Organic Geochemistry* **1999**, 30, (12), 1479-1493.
25. Cho, J. M.; Davis, J. M.; Huber, G. W., The Intrinsic Kinetics and Heats of Reactions for Cellulose Pyrolysis and Char Formation. *ChemSusChem* **2010**, 3, (10), 1162-1165.
26. Broido, A.; Nelson, M. A., Char yield on pyrolysis of cellulose. *Combustion and Flame* **1975**, 24, (2), 263-268.
27. Lewellen, P. C.; Peters, W. A.; Howard, J. B., Cellulose pyrolysis kinetics and char formation mechanism. *International Symposium on Combustion* **1977**, 16, (1), 1471-1480.
28. Bradbury, A. G. W.; Sakai, Y.; Shafizadeh, F., Kinetic model for pyrolysis of cellulose. *Journal of Applied Polymer Science* **1979**, 23, (11), 3271-3280.
29. Hopkins, M. W.; DeJenga, C.; Antal, M. J., The flash pyrolysis of cellulosic materials using concentrated visible light. *Solar Energy* **1984**, 32, (4), 547-551.

30. Diebold, J. P., A unified, global model for the pyrolysis of cellulose. *Biomass & Bioenergy* **1994**, 7, (1-6), 75-85.
31. Banyasz, J. L.; Li, S.; Lyons-Hart, J. L.; Shafer, K. H., Cellulose pyrolysis: the kinetics of hydroxyacetaldehyde evolution. *Journal of Analytical and Applied Pyrolysis* **2001**, 57, (2), 223-248.
32. Onay, O.; Kockar, O. M., Slow, fast and flash pyrolysis of rapeseed. *Renewable Energy* **2003**, 28, (15), 2417-2433.
33. Proano-Aviles, J.; Lindstrom, J. K.; Johnston, P. A.; Brown, R. C., Heat and Mass Transfer Effects in a Furnace-Based Micropyrolyzer. *Energy Technology* **2017**, 5, (1), 189-195.
34. Zhang, H. Y.; Xiao, R.; Huang, H.; Xiao, G., Comparison of non-catalytic and catalytic fast pyrolysis of corncob in a fluidized bed reactor. *Bioresource Technology* **2009**, 100, (3), 1428-1434.
35. Molga, E. J.; van Woezik, B. A. A.; Westerterp, K. R., Neural networks for modelling of chemical reaction systems with complex kinetics: oxidation of 2-octanol with nitric acid. *Chemical Engineering and Processing* **2000**, 39, (4), 323-334.
36. Puig-Arnabat, M.; Hernandez, J. A.; Bruno, J. C.; Coronas, A., Artificial neural network models for biomass gasification in fluidized bed gasifiers. *Biomass & Bioenergy* **2013**, 49, 279-289.
37. Molga, E. J., Neural network approach to support modelling of chemical reactors: problems, resolutions, criteria of application. *Chemical Engineering and Processing* **2003**, 42, (8-9), 675-695.

38. Dong, Z. J.; Yang, Y.; Cai, W. F.; He, Y. F.; Chai, M. Y.; Liu, B. B.; Yu, X.; Banks, S. W.; Zhang, X. G.; Bridgwater, A. V.; Cai, J. M., Theoretical Analysis of Double Logistic Distributed Activation Energy Model for Thermal Decomposition Kinetics of Solid Fuels. *Industrial & Engineering Chemistry Research* **2018**, 57, (23), 7817-7825.
39. Alves, S. S.; Figueiredo, J. L., Pyrolysis kinetics of lignocellulosic materials by multistage isothermal thermogravimetry. *Journal of Analytical and Applied Pyrolysis* **1988**, 13, (1-2), 123-134.
40. Mamleev, V.; Bourbigot, S.; Le Bras, M.; Yvon, J., The facts and hypotheses relating to the phenomenological model of cellulose pyrolysis Interdependence of the steps. *Journal of Analytical and Applied Pyrolysis* **2009**, 84, (1), 1-17.
41. Dalluge, D.; Whitmer, L. E.; Polin, J. P.; Yong, S. C.; Shanks, B. H.; Brown, R. C., Comparison of direct and indirect contact heat exchange to improve recovery of bio-oil. *Applied Energy* **2019**, 251, (1), 1-10.
42. Varhegyi, G.; Antal, M. J.; Jakab, E.; Szabo, P., Kinetic modeling of biomass pyrolysis. *Journal of Analytical and Applied Pyrolysis* **1997**, 42, (1), 73-87.
43. Anca-Couce, A., Reaction mechanisms and multi-scale modelling of lignocellulosic biomass pyrolysis. *Progress in Energy and Combustion Science* **2016**, 53, 41-79.
44. Anca-Couce, A.; Mehrabian, R.; Scharler, R.; Obernberger, I., Kinetic scheme of biomass pyrolysis considering secondary charring reactions. *Energy Conversion and Management* **2014**, 87, 687-696.

45. Wang, S. R.; Dai, G. X.; Yang, H. P.; Luo, Z. Y., Lignocellulosic biomass pyrolysis mechanism: A state-of-the-art review. *Progress in Energy and Combustion Science* **2017**, 62, 33-86.
46. Dhyani, V.; Bhaskar, T., A comprehensive review on the pyrolysis of lignocellulosic biomass. *Renewable Energy* **2018**, 129, 695-716.
47. Zhou, X.; Li, W.; Mabon, R.; Broadbelt, L. J., A Critical Review on Hemicellulose Pyrolysis. *Energy Technology* **2017**, 5, (1), 52-79.
48. Choi, M. K.; Park, H. C.; Choi, H. S., Comprehensive evaluation of various pyrolysis reaction mechanisms for pyrolysis process simulation. *Chem. Eng. Process.* **2018**, 130, 19-35.
49. Mohan, D.; Pittman, C. U.; Steele, P. H., Pyrolysis of wood/biomass for bio-oil: A critical review. *Energy & Fuels* **2006**, 20, (3), 848-889.
50. Huard, M.; Briens, C.; Berruti, F.; Gauthier, T. A., A Review of Rapid Gas-Solid Separation Techniques. *International Journal of Chemical Reactor Engineering* **2010**, 8, 1-75.
51. Bridgwater, A. V., Review of fast pyrolysis of biomass and product upgrading. *Biomass & Bioenergy* **2012**, 38, 68-94.
52. Bridgwater, A., Fast pyrolysis of biomass for the production of liquids. In *Biomass Combustion Science, Technology and Engineering*, Rosendahl, L., Ed. 2013; pp 130-171.
53. Bridgwater, T., Challenges and Opportunities in Fast Pyrolysis of Biomass: Part II Upgrading options and promising applications in energy, biofuels and chemicals. *Johnson Matthey Technology Review* **2018**, 62, (2), 150-160.

54. Czernik, S.; Bridgwater, A. V., Overview of applications of biomass fast pyrolysis oil. *Energy & Fuels* **2004**, 18, (2), 590-598.
55. Di Blasi, C., Modeling chemical and physical processes of wood and biomass pyrolysis. *Progress in Energy and Combustion Science* **2008**, 34, (1), 47-90.
56. Butler, E.; Devlin, G.; Meier, D.; McDonnell, K., A review of recent laboratory research and commercial developments in fast pyrolysis and upgrading. *Renewable & Sustainable Energy Reviews* **2011**, 15, (8), 4171-4186.
57. Carpenter, D.; Westover, T. L.; Czernik, S.; Jablonski, W., Biomass feedstocks for renewable fuel production: a review of the impacts of feedstock and pretreatment on the yield and product distribution of fast pyrolysis bio-oils and vapors. *Green Chemistry* **2014**, 16, (2), 384-406.
58. Dickerson, T.; Soria, J., Catalytic Fast Pyrolysis: A Review. *Energies* **2013**, 6, (1), 514-538.
59. Jiang, J.; Xu, J.; Song, Z., Review of the direct thermochemical conversion of lignocellulosic biomass for liquid fuels. *Frontiers of Agricultural Science and Engineering* **2015**, 2, (1), 13-27.
60. Sharma, A.; Pareek, V.; Zhang, D. K., Biomass pyrolysis-A review of modelling, process parameters and catalytic studies. *Renewable & Sustainable Energy Reviews* **2015**, 50, 1081-1096.
61. Mostafazadeh, A. K.; Solomatnikova, O.; Drogui, P.; Tyagi, R. D., A review of recent research and developments in fast pyrolysis and bio-oil upgrading. *Biomass Conversion and Biorefinery* **2018**, 8, (3), 739-773.

62. Hameed, S.; Sharma, A.; Pareek, V.; Wu, H. W.; Yu, Y., A review on biomass pyrolysis models: Kinetic, network and mechanistic models. *Biomass & Bioenergy* **2019**, 123, 104-122.
63. Mettler, M. S.; Mushrif, S. H.; Paulsen, A. D.; Javadkar, A. D.; Vlachos, D. G.; Dauenhauer, P. J., Revealing pyrolysis chemistry for biofuels production: Conversion of cellulose to furans and small oxygenates. *Energy & Environmental Science* **2012**, 5, (1), 5414-5424.
64. Mettler, M. S.; Paulsen, A. D.; Vlachos, D. G.; Dauenhauer, P. J., The chain length effect in pyrolysis: bridging the gap between glucose and cellulose. *Green Chemistry* **2012**, 14, (5), 1284-1288.
65. Mettler, M. S.; Paulsen, A. D.; Vlachos, D. G.; Dauenhauer, P. J., Pyrolytic conversion of cellulose to fuels: levoglucosan deoxygenation via elimination and cyclization within molten biomass. *Energy & Environmental Science* **2012**, 5, (7), 7864-7868.
66. Lindstrom, J. K.; Proano-Aviles, J.; Johnston, P. A.; Peterson, C. A.; Stansell, J. S.; Brown, R. C., Competing reactions limit levoglucosan yield during fast pyrolysis of cellulose. *Green Chemistry* **2019**, 21, (1), 178-186.
67. Capart, R.; Khezami, L.; Burnham, A. K., Assessment of various kinetic models for the pyrolysis of a microgranular cellulose. *Thermochimica Acta* **2004**, 417, (1), 79-89.
68. Wang, S. R.; Liu, Q.; Liao, Y. F.; Luo, Z. Y.; Cen, K. F., A study on the mechanism research on cellulose pyrolysis under catalysis of metallic salts. *Korean Journal of Chemical Engineering* **2007**, 24, (2), 336-340.
69. Gao, Z. X.; Li, N.; Chen, M.; Yi, W. M., Comparative study on the pyrolysis of cellulose and its model compounds. *Fuel Processing Technology* **2019**, 193, 131-140.

70. Burnham, A. K.; Zhou, X. W.; Broadbelt, L. J., Critical Review of the Global Chemical Kinetics of Cellulose Thermal Decomposition. *Energy & Fuels* **2015**, 29, (5), 2906-2918.
71. Oja, V.; Suuberg, E. M., Vapor pressures and enthalpies of sublimation of D-glucose, D-xylose, cellobiose, and levoglucosan. *Journal of Chemical and Engineering Data* **1999**, 44, (1), 26-29.
72. Zhang, J.; Nolte, M. W.; Shanks, B. H., Investigation of Primary Reactions and Secondary Effects from the Pyrolysis of Different Celluloses. *ACS Sustainable Chemistry & Engineering* **2014**, 2, (12), 2820-2830.
73. Teixeira, A. R.; Mooney, K. G.; Kruger, J. S.; Williams, C. L.; Suszynski, W. J.; Schmidt, L. D.; Schmidt, D. P.; Dauenhauer, P. J., Aerosol generation by reactive boiling ejection of molten cellulose. *Energy & Environmental Science* **2011**, 4, (10), 4306-4321.
74. Jegers, H. E.; Klein, M. T., Primary and secondary lignin pyrolysis reaction pathways. *Industrial & Engineering Chemistry Process Design and Development* **1985**, 24, (1), 173-183.
75. Caballero, J. A.; Font, R.; Marcilla, A., Pyrolysis of Kraft lignin: Yields and correlations. *Journal of Analytical and Applied Pyrolysis* **1997**, 39, (2), 161-183.
76. Hilbers, T. J.; Wang, Z. H.; Pecha, B.; Westerhof, R. J. M.; Kersten, S. R. A.; Pelaez-Samaniego, M. R.; Garcia-Perez, M., Cellulose-Lignin interactions during slow and fast pyrolysis. *Journal of Analytical and Applied Pyrolysis* **2015**, 114, 197-207.
77. Laskar, D. D.; Yang, B.; Wang, H.; Lee, J., Pathways for biomass-derived lignin to hydrocarbon fuels. *Biofuels Bioproducts & Biorefining* **2013**, 7, (5), 602-626.

78. Prasomsri, T.; Shetty, M.; Murugappan, K.; Roman-Leshkov, Y., Insights into the catalytic activity and surface modification of MoO₃ during the hydrodeoxygenation of lignin-derived model compounds into aromatic hydrocarbons under low hydrogen pressures. *Energy & Environmental Science* **2014**, 7, (8), 2660-2669.
79. Anderson, E. M.; Katahira, R.; Reed, M.; Resch, M. G.; Karp, E. M.; Beckham, G. T.; Roman-Leshkov, Y., Reductive Catalytic Fractionation of Corn Stover Lignin. *ACS Sustainable Chemistry & Engineering* **2016**, 4, (12), 6940-6950.
80. Anderson, E.; Crisci, A.; Murugappan, K.; Roman-Leshkov, Y., Bifunctional Molybdenum Polyoxometalates for the Combined Hydrodeoxygenation and Alkylation of Lignin-Derived Model Phenolics. *ChemSusChem* **2017**, 10, (10), 2226-2234.
81. Anderson, E. M.; Stone, M. L.; Katahira, R.; Reed, M.; Muchero, W.; Ramirez, K. J.; Beckham, G. T.; Román-Leshkov, Y., Differences in S/G ratio in natural poplar variants do not predict catalytic depolymerization monomer yields. *Nature Communications* **2019**, 10, (1), 2033-2043.
82. Ciddor, L.; Bennett, J. A.; Hunns, J. A.; Wilson, K.; Lee, A. F., Catalytic upgrading of bio-oils by esterification. *Journal of Chemical Technology and Biotechnology* **2015**, 90, (5), 780-795.
83. Elliott, D. C., Biofuel from fast pyrolysis and catalytic hydrodeoxygenation. *Current Opinion in Chemical Engineering* **2015**, 9, 59-65.
84. Ko, C. H.; Park, S. H.; Jeon, J.-K.; Suh, D. J.; Jeong, K.-E.; Park, Y.-K., Upgrading of biofuel by the catalytic deoxygenation of biomass. *Korean Journal of Chemical Engineering* **2012**, 29, (12), 1657-1665.

85. Nga, T.; Uemura, Y.; Chowdhury, S.; Ramli, A., A review of bio-oil upgrading by catalytic hydrodeoxygenation. In *Process and Advanced Materials Engineering*, Ahmed, I., Ed. 2014; Vol. 625, pp 255-258.
86. Liao, H.; Ye, X.; Lu, Q.; Dong, C., Overview of Bio-oil Upgrading Via Catalytic Cracking. In *Solar Energy Materials and Energy Engineering*, Feng, X.; Luo, Q.; Zhang, T., Eds. 2014; Vol. 827, pp 25-29.
87. Mortensen, P. M.; Grunwaldt, J. D.; Jensen, P. A.; Knudsen, K. G.; Jensen, A. D., A review of catalytic upgrading of bio-oil to engine fuels. *Applied Catalysis a-General* **2011**, 407, (1-2), 1-19.
88. Pogaku, R.; Hardinge, B. S.; Vuthaluru, H.; Amir, H. A., Production of bio-oil from oil palm empty fruit bunch by catalytic fast pyrolysis: a review. *Biofuels-UK* **2016**, 7, (6), 647-660.
89. Tan, S.; Zhang, Z.; Sun, J.; Wang, Q., Catalysts in Biomass Pyrolysis: A Brief Review. In *Progress in Renewable and Sustainable Energy, Pts 1 and 2*, Li, Y. G.; Li, Y.; Pan, W. G., Eds. 2013; Vol. 608-609, pp 428-432.
90. Zhang, L.; Liu, R.; Yin, R.; Mei, Y., Upgrading of bio-oil from biomass fast pyrolysis in China: A review. *Renewable & Sustainable Energy Reviews* **2013**, 24, 66-72.
91. Sharifzadeh, M.; Richard, C. J.; Shah, N., Modelling the kinetics of pyrolysis oil hydrothermal upgrading based on the connectivity of oxygen atoms, quantified by P-31-NMR. *Biomass & Bioenergy* **2017**, 98, 272-290.
92. Paine, J. B.; Pithawalla, Y. B.; Naworal, J. D.; Thomas, C. E., Carbohydrate pyrolysis mechanisms from isotopic labeling. Part 1. The pyrolysis of glycerin: Discovery of competing

fragmentation mechanisms affording acetaldehyde and formaldehyde and the implications for carbohydrate pyrolysis. *Journal of Analytical and Applied Pyrolysis* **2007**, 80, (2), 297-311.

93. Paine, J. B.; Pithawalla, Y. B.; Naworal, J. D., Carbohydrate pyrolysis mechanisms from isotopic labeling. Part 5. The pyrolysis of D-glucose: The origin of the light gases from the D-glucose molecule. *Journal of Analytical and Applied Pyrolysis* **2019**, 138, 70-93.

94. Paine, J. B.; Pithawalla, Y. B.; Naworal, J. D., Carbohydrate pyrolysis mechanisms from isotopic labeling. Part 3. The Pyrolysis of D-glucose: Formation of C-3 and C-4 carbonyl compounds and a cyclopentenedione isomer by electrocyclic fragmentation mechanisms. *Journal of Analytical and Applied Pyrolysis* **2008**, 82, (1), 42-69.

95. Paine, J. B.; Pithawalla, Y. B.; Naworal, J. D., Carbohydrate pyrolysis mechanisms from isotopic labeling. Part 2. The pyrolysis of D-glucose: General disconnective analysis and the formation of C-1 and C-2 carbonyl compounds by electrocyclic fragmentation mechanisms. *Journal of Analytical and Applied Pyrolysis* **2008**, 82, (1), 10-41.

96. Paine, J. B.; Pithawalla, Y. B.; Naworal, J. D., Carbohydrate pyrolysis mechanisms from isotopic labeling. Part 4. The pyrolysis Of D-glucose: The formation of furans. *Journal of Analytical and Applied Pyrolysis* **2008**, 83, (1), 37-63.

97. Mushrif, S. H.; Vasudevan, V.; Krishnamurthy, C. B.; Venkatesh, B., Multiscale molecular modeling can be an effective tool to aid the development of biomass conversion technology: A perspective. *Chemical Engineering Science* **2015**, 121, 217-235.

- 1
2
3 98. Laio, A.; Gervasio, F. L., Metadynamics: a method to simulate rare events and reconstruct
4 the free energy in biophysics, chemistry and material science. *Reports on Progress in Physics*
5
6 **2008**, 71, (12).
7
8
9
10
11 99. Mayes, H. B.; Broadbelt, L. J., Unraveling the Reactions that Unravel Cellulose. *Journal*
12
13 *of Physical Chemistry A* **2012**, 116, (26), 7098-7106.
14
15
16 100. Assary, R. S.; Curtiss, L. A., Comparison of Sugar Molecule Decomposition through
17
18 Glucose and Fructose: A High-Level Quantum Chemical Study. *Energy & Fuels* **2012**, 26, (2),
19
20 1344-1352.
21
22
23 101. Assary, R. S.; Curtiss, L. A., Thermochemistry and Reaction Barriers for the Formation of
24
25 Levoglucosenone from Cellobiose. *Chemcatchem* **2012**, 4, (2), 200-205.
26
27
28 102. Seshadri, V.; Westmoreland, P. R., Roles of hydroxyls in the noncatalytic and catalyzed
29
30 formation of levoglucosan from glucose. *Catalysis Today* **2016**, 269, 110-121.
31
32
33 103. Seshadri, V.; Westmoreland, P. R., Concerted Reactions and Mechanism of Glucose
34
35 Pyrolysis and Implications for Cellulose Kinetics. *Journal of Physical Chemistry A* **2012**, 116,
36
37 (49), 11997-12013.
38
39
40 104. Huang, J. B.; Liu, C.; Wei, S. N.; Huang, X. L.; Li, H. J., Density functional theory studies
41
42 on pyrolysis mechanism of beta-D-glucopyranose. *Journal of Molecular Structure-Theochem*
43
44 **2010**, 958, (1-3), 64-70.
45
46
47 105. Hu, B.; Lu, Q.; Wu, Y. T.; Zhang, Z. X.; Cui, M. S.; Liu, D. J.; Dong, C. Q.; Yang, Y. P.,
48
49 Catalytic mechanism of sulfuric acid in cellulose pyrolysis: A combined experimental and
50
51 computational investigation. *Journal of Analytical and Applied Pyrolysis* **2018**, 134, 183-194.
52
53
54
55
56
57
58
59
60

106. Liu, C.; Huang, J. B.; Huang, X. L.; Li, H. J.; Zhang, Z., Theoretical studies on formation mechanisms of CO and CO₂ in cellulose pyrolysis. *Computational and Theoretical Chemistry* **2011**, 964, (1-3), 207-212.
107. Hosoya, T.; Kawamoto, H.; Saka, S., Secondary reactions of lignin-derived primary tar components. *Journal of Analytical and Applied Pyrolysis* **2008**, 83, (1), 78-87.
108. Agarwal, V.; Dauenhauer, P. J.; Huber, G. W.; Auerbach, S. M., Ab Initio Dynamics of Cellulose Pyrolysis: Nascent Decomposition Pathways at 327 and 600 degrees C. *Journal of the American Chemical Society* **2012**, 134, (36), 14958-14972.
109. Maliekkal, V.; Maduskar, S.; Saxon, D. J.; Nasiri, M.; Reineke, T. M.; Neurock, M.; Dauenhauer, P., Activation of Cellulose via Cooperative Hydroxyl-Catalyzed Transglycosylation of Glycosidic Bonds. *ACS Catalysis* **2019**, 9, (3), 1943-1955.
110. Zhou, X. W.; Nolte, M. W.; Mayes, H. B.; Shanks, B. H.; Broadbelt, L. J., Experimental and Mechanistic Modeling of Fast Pyrolysis of Neat Glucose-Based Carbohydrates. 1. Experiments and Development of a Detailed Mechanistic Model. *Industrial & Engineering Chemistry Research* **2014**, 53, (34), 13274-13289.
111. Mayes, H. B.; Nolte, M. W.; Beckham, G. T.; Shanks, B. H.; Broadbelt, L. J., The Alpha-Bet(a) of Glucose Pyrolysis: Computational and Experimental Investigations of 5-Hydroxymethylfurfural and Levoglucosan Formation Reveal Implications for Cellulose Pyrolysis. *ACS Sustainable Chemistry & Engineering* **2014**, 2, (6), 1461-1473.
112. Mayes, H. B.; Tian, J. H.; Nolte, M. W.; Shanks, B. H.; Beckham, G. T.; Gnanakaran, S.; Broadbelt, L. J., Sodium Ion Interactions with Aqueous Glucose: Insights from Quantum

Mechanics, Molecular Dynamics, and Experiment. *Journal of Physical Chemistry B* **2014**, 118, (8), 1990-2000.

113. Mayes, H. B.; Nolte, M. W.; Beckham, G. T.; Shanks, B. H.; Broadbelt, L. J., The Alpha-Bet(a) of Salty Glucose Pyrolysis: Computational Investigations Reveal Carbohydrate Pyrolysis Catalytic Action by Sodium Ions. *ACS Catalysis* **2015**, 5, (1), 192-202.

114. Wang, M.; Liu, C.; Li, Q. B.; Xu, X. X., Theoretical insight into the conversion of xylose to furfural in the gas phase and water. *Journal of Molecular Modeling* **2015**, 21, (11).

115. Huang, J. B.; He, C.; Wu, L. Q.; Tong, H., Thermal degradation reaction mechanism of xylose: A DFT study. *Chemical Physics Letters* **2016**, 658, 114-124.

116. Huang, J. B.; Liu, C.; Tong, H.; Li, W. M.; Wu, D., Theoretical studies on pyrolysis mechanism of xylopyranose. *Computational and Theoretical Chemistry* **2012**, 1001, 44-50.

117. Huang, X. Y.; Cheng, B. G.; Chen, F. Q.; Zhan, X. L., Reaction pathways of hemicellulose and mechanism of biomass pyrolysis in hydrogen plasma: A density functional theory study. *Renewable Energy* **2016**, 96, 490-497.

118. Wang, S. R.; Ru, B.; Lin, H. Z.; Luo, Z. Y., Degradation mechanism of monosaccharides and xylan under pyrolytic conditions with theoretic modeling on the energy profiles. *Bioresource Technology* **2013**, 143, 378-383.

119. Wang, S. R.; Ru, B.; Lin, H. Z.; Sun, W. X.; Yu, C. J.; Luo, Z. Y., Pyrolysis Mechanism of Hemicellulose Monosaccharides in Different Catalytic Processes. *Chemical Research in Chinese Universities* **2014**, 30, (5), 848-854.

120. Li, Z. Y.; Liu, C.; Xu, X. X.; Li, Q. B., A theoretical study on the mechanism of xylobiose during pyrolysis process. *Computational and Theoretical Chemistry* **2017**, 1117, 130-140.

121. Hu, B.; Lu, Q.; Zhang, Z. X.; Wu, Y. T.; Li, K.; Dong, C. Q.; Yang, Y. P., Mechanism insight into the fast pyrolysis of xylose, xylobiose and xylan by combined theoretical and experimental approaches. *Combustion and Flame* **2019**, 206, 177-188.

122. Khachatryan, L.; Asatryan, R.; McFerrin, C.; Adoukpe, J.; Dellinger, B., Radicals from the Gas-Phase Pyrolysis of Catechol. 2. Comparison of the Pyrolysis of Catechol and Hydroquinone. *Journal of Physical Chemistry A* **2010**, 114, (37), 10110-10116.

123. Huang, J. B.; Liu, C.; Wu, D.; Tong, H.; Ren, L. R., Density functional theory studies on pyrolysis mechanism of beta-O-4 type lignin dimer model compound. *Journal of Analytical and Applied Pyrolysis* **2014**, 109, 98-108.

124. Zhang, J. J.; Jiang, X. Y.; Ye, X. N.; Chen, L.; Lu, Q.; Wang, X. H.; Dong, C. Q., Pyrolysis mechanism of a beta-O-4 type lignin dimer model compound. *Journal of Thermal Analysis and Calorimetry* **2016**, 123, (1), 501-510.

125. Li, S. M.; Luo, Z. Y.; Wang, W. B.; Lu, K. Y.; Yang, Y.; Liang, X. R., Characterization of pyrolytic lignin and insight into its formation mechanisms using novel techniques and DFT method. *Fuel* **2020**, 262.

126. da Silva, G.; Bozzelli, J. W., Quantum chemical study of the thermal decomposition of o-quinone methide (6-methylene-2,4-cyclohexadien-1-one). *Journal of Physical Chemistry A* **2007**, 111, (32), 7987-7994.

127. Asatryan, R.; Hudzik, J. M.; Bozzelli, J. W.; Khachatryan, L.; Ruckenstein, E., OH-Initiated Reactions of p-Coumaryl Alcohol Relevant to the Lignin Pyrolysis. Part I. Potential Energy Surface Analysis. *Journal of Physical Chemistry A* **2019**, 123, (13), 2570-2585.
128. Shaw, A.; Zhang, X. L., Density functional study on the thermal stabilities of phenolic bio-oil compounds. *Fuel* **2019**, 255.
129. Cao, Y. Z.; Tang, M.; Yang, P.; Chen, M. Z.; Wang, S. Q.; Hua, H. M.; Chen, W. M.; Zhou, X. Y., Atmospheric Low-Temperature Plasma-Induced Changes in the Structure of the Lignin Macromolecule: An Experimental and Theoretical Investigation. *Journal of Agricultural and Food Chemistry* **2020**, 68, (2), 451-460.
130. Chen, L.; Ye, X. N.; Luo, F. X.; Shao, J. G.; Lu, Q.; Fang, Y.; Wang, X. H.; Chen, H. P., Pyrolysis mechanism of beta-O-4 type lignin model dimer. *Journal of Analytical and Applied Pyrolysis* **2015**, 115, 103-111.
131. Hu, Y. M.; Zuo, L.; Liu, J. Y.; Sun, J. Y.; Wu, S. B., Chemical Simulation and Quantum Chemical Calculation of Lignin Model Compounds. *Bioresources* **2016**, 11, (1), 1044-1060.
132. Liu, C.; Deng, Y. B.; Wu, S. B.; Lei, M.; Liang, J. J., Experimental and Theoretical Analysis of the Pyrolysis Mechanism of a Dimeric Lignin Model Compound with alpha-O-4 Linkage. *Bioresources* **2016**, 11, (2), 3626-3636.
133. Liu, C.; Zhang, Y. Y.; Huang, X. L., Study of guaiacol pyrolysis mechanism based on density function theory. *Fuel Processing Technology* **2014**, 123, 159-165.

134. Huang, J. B.; He, C.; Liu, C.; Tong, H.; Wu, L. Q.; Wu, S. B., A computational study on thermal decomposition mechanism of beta-1 linkage lignin dimer. *Computational and Theoretical Chemistry* **2015**, 1054, 80-87.
135. Liu, C.; Deng, Y. B.; Wu, S. B.; Mou, H. Y.; Liang, J. J.; Lei, M., Study on the pyrolysis mechanism of three guaiacyl-type lignin monomeric model compounds. *Journal of Analytical and Applied Pyrolysis* **2016**, 118, 123-129.
136. Huang, J. B.; He, C., Pyrolysis mechanism of alpha-O-4 linkage lignin dimer: A theoretical study. *Journal of Analytical and Applied Pyrolysis* **2015**, 113, 655-664.
137. Jiang, X. Y.; Lu, Q.; Ye, X. N.; Hu, B.; Dong, C. Q., Experimental and Theoretical Studies on the Pyrolysis Mechanism of beta-1-Type Lignin Dimer Model Compound. *Bioresources* **2016**, 11, (3), 6232-6243.
138. Jiang, X. Y.; Lu, Q.; Hu, B.; Liu, J.; Dong, C. Q.; Yang, Y. P., Intermolecular interaction mechanism of lignin pyrolysis: A joint theoretical and experimental study. *Fuel* **2018**, 215, 386-394.
139. Younker, J. M.; Beste, A.; Buchanan, A. C., Computational Study of Bond Dissociation Enthalpies for Substituted ss-O-4 Lignin Model Compounds. *Chemphyschem* **2011**, 12, (18), 3556-3565.
140. Beste, A.; Buchanan, A. C., Computational Study of Bond Dissociation Enthalpies for Lignin Model Compounds. Substituent Effects in Phenethyl Phenyl Ethers. *Journal of Organic Chemistry* **2009**, 74, (7), 2837-2841.

141. Younker, J. M.; Beste, A.; Buchanan, A. C., Computational study of bond dissociation enthalpies for lignin model compounds: beta-5 Arylcoumaran. *Chemical Physics Letters* **2012**, 545, 100-106.

142. Parthasarathi, R.; Romero, R. A.; Redondo, A.; Gnanakaran, S., Theoretical Study of the Remarkably Diverse Linkages in Lignin. *Journal of Physical Chemistry Letters* **2011**, 2, (20), 2660-2666.

143. Sheng, H. M.; Murria, P.; Degenstein, J. C.; Tang, W. J.; Riedeman, J. S.; Hurt, M. R.; Dow, A.; Klein, I.; Zhu, H. Y.; Nash, J. J.; Abu-Omar, M.; Agrawal, R.; Delgass, W. N.; Ribeiro, F. H.; Kenttamaa, H. I., Initial Products and Reaction Mechanisms for Fast Pyrolysis of Synthetic G-Lignin Oligomers with beta-O-4 Linkages via On-Line Mass Spectrometry and Quantum Chemical Calculations. *Chemistryselect* **2017**, 2, (24), 7185-7193.

144. Furutani, Y.; Dohara, Y.; Kudo, S.; Hayashi, J.; Norinaga, K., Theoretical Study on the Kinetics of Thermal Decomposition of Guaiacol and Catechol. *Journal of Physical Chemistry A* **2017**, 121, (44), 8495-8503.

145. Altarawneh, M.; Dlugogorski, B. Z.; Kennedy, E. M.; Mackie, J. C., Theoretical Study of Unimolecular Decomposition of Catechol. *Journal of Physical Chemistry A* **2010**, 114, (2), 1060-1067.

146. Altarawneh, M.; Dlugogorski, B. Z.; Kennedy, E. M.; Mackie, J. C., Thermochemical Properties and Decomposition Pathways of Three Isomeric Semiquinone Radicals. *Journal of Physical Chemistry A* **2010**, 114, (2), 1098-1108.

147. Dellon, L. D.; Yanez, A. J.; Li, W. J.; Mabon, R.; Broadbelt, L. J., Computational Generation of Lignin Libraries from Diverse Biomass Sources. *Energy & Fuels* **2017**, 31, (8), 8263-8274.
148. Faravelli, T.; Frassoldati, A.; Hemings, E. B.; Ranzi, E., Multistep Kinetic Model of Biomass Pyrolysis. In *Cleaner Combustion: Developing Detailed Chemical Kinetic Models*, Battin-Leclerc, F.; Simmie, J. M.; Blurock, E., Eds. 2013; pp 111-139.
149. Patwardhan, P. R.; Dalluge, D. L.; Shanks, B. H.; Brown, R. C., Distinguishing primary and secondary reactions of cellulose pyrolysis. *Bioresource Technology* **2011**, 102, (8), 5265-5269.
150. Patwardhan, P. R.; Satrio, J. A.; Brown, R. C.; Shanks, B. H., Product distribution from fast pyrolysis of glucose-based carbohydrates. *Journal of Analytical and Applied Pyrolysis* **2009**, 86, (2), 323-330.
151. Hosoya, T.; Kawamoto, H.; Saka, S., Secondary reactions of lignin-derived primary tar components. *Journal of Analytical and Applied Pyrolysis* **2008**, 83, (1), 78-87.
152. Milosavljevic, I.; Oja, V.; Suuberg, E. M., Thermal effects in cellulose pyrolysis: Relationship to char formation processes. *Industrial & Engineering Chemistry Research* **1996**, 35, (3), 653-662.
153. Milosavljevic, I.; Suuberg, E. M., Cellulose thermal-decomposition kinetics - global mass-loss kinetics. *Industrial & Engineering Chemistry Research* **1995**, 34, (4), 1081-1091.
154. Azeez, A. M.; Meier, D.; Odermatt, J.; Willner, T., Fast Pyrolysis of African and European Lignocellulosic Biomasses Using Py-GC/MS and Fluidized Bed Reactor. *Energy & Fuels* **2010**, 24, (3), 2078-2085.

155. Zhou, X. W.; Nolte, M. W.; Shanks, B. H.; Broadbelt, L. J., Experimental and Mechanistic Modeling of Fast Pyrolysis of Neat Glucose-Based Carbohydrates. 2. Validation and Evaluation of the Mechanistic Model. *Industrial & Engineering Chemistry Research* **2014**, 53, (34), 13290-13301.
156. Patwardhan, P. R.; Brown, R. C.; Shanks, B. H., Product Distribution from the Fast Pyrolysis of Hemicellulose. *Chemsuschem* **2011**, 4, (5), 636-643.
157. Dalluge, D. L.; Daugaard, T.; Johnston, P.; Kuzhiyil, N.; Wright, M. M.; Brown, R. C., Continuous production of sugars from pyrolysis of acid-infused lignocellulosic biomass. *Green Chemistry* **2014**, 16, (9), 4144-4155.
158. Ren, T. Y.; Qi, W.; Su, R. X.; He, Z. M., Promising Techniques for Depolymerization of Lignin into Value-added Chemicals. *Chemcatchem* **2019**, 11, (2), 639-654.
159. Lin, Y. C.; Cho, J.; Tompsett, G. A.; Westmoreland, P. R.; Huber, G. W., Kinetics and Mechanism of Cellulose Pyrolysis. *Journal of Physical Chemistry C* **2009**, 113, (46), 20097-20107.
160. Shafizadeh, F.; Stevenson, T. T.; Cochran, T. G.; Furneaux, R. H., 1,5-anhydro-4-deoxy-D-glycero-hex-1-en-3-ulose and other pyrolysis products of cellulose. *Carbohydrate Research* **1978**, 67, (2), 433-447.
161. Raveendran, K.; Ganesh, A.; Khilar, K. C., Influence of mineral matter on biomass pyrolysis characteristics. *Fuel* **1995**, 74, (12), 1812-1822.

162. Wang, J.; Zhang, M. Q.; Chen, M. Q.; Min, F. F.; Zhang, S. P.; Ren, Z. W.; Yan, Y. J., Catalytic effects of six inorganic compounds on pyrolysis of three kinds of biomass. *Thermochimica Acta* **2006**, 444, (1), 110-114.
163. Trendewicz, A.; Evans, R.; Dutta, A.; Sykes, R.; Carpenter, D.; Braun, R., Evaluating the effect of potassium on cellulose pyrolysis reaction kinetics. *Biomass & Bioenergy* **2015**, 74, 15-25.
164. Papari, S.; Hawboldt, K., A review on the pyrolysis of woody biomass to bio-oil: Focus on kinetic models. *Renewable & Sustainable Energy Reviews* **2015**, 52, 1580-1595.
165. Di Blasi, C., Modelling the fast pyrolysis of cellulosic particles in fluid-bed reactors. *Chemical Engineering Science* **2000**, 55, (24), 5999-6013.
166. White, J. E.; Catallo, W. J.; Legendre, B. L., Biomass pyrolysis kinetics: A comparative critical review with relevant agricultural residue case studies. *Journal of Analytical and Applied Pyrolysis* **2011**, 91, (1), 1-33.
167. Raveendran, K.; Ganesh, A.; Khilar, K. C., Pyrolysis characteristics of biomass and biomass components. *Fuel* **1996**, 75, (8), 987-998.
168. Wang, G.; Li, W.; Li, B. Q.; Chen, H. K., TG study on pyrolysis of biomass and its three components under syngas. *Fuel* **2008**, 87, (4-5), 552-558.
169. Wang, S. R.; Guo, X. J.; Wang, K. G.; Luo, Z. Y., Influence of the interaction of components on the pyrolysis behavior of biomass. *Journal of Analytical and Applied Pyrolysis* **2011**, 91, (1), 183-189.

170. Worasuwanarak, N.; Sonobe, T.; Tanthapanichakoon, W., Pyrolysis behaviors of rice straw, rice husk, and corncob by TG-MS technique. *Journal of Analytical and Applied Pyrolysis* **2007**, 78, (2), 265-271.

171. Yang, H. P.; Yan, R.; Chen, H. P.; Zheng, C. G.; Lee, D. H.; Liang, D. T., In-depth investigation of biomass pyrolysis based on three major components: Hemicellulose, cellulose and lignin. *Energy & Fuels* **2006**, 20, (1), 388-393.

172. Cai, J. M.; Xu, D.; Dong, Z. J.; Yu, X.; Yang, Y.; Banks, S. W.; Bridgwater, A. V., Processing thermogravimetric analysis data for isoconversional kinetic analysis of lignocellulosic biomass pyrolysis: Case study of corn stalk. *Renewable & Sustainable Energy Reviews* **2018**, 82, 2705-2715.

173. Brown, M. E., Steps in a minefield - Some kinetic aspects of thermal analysis. *Journal of Thermal Analysis* **1997**, 49, (1), 17-32.

174. Galwey, A. K.; Brown, M. E., A Theoretical justification for the application of the arrhenius equation to kinetics of solid-state reactions (Mainly ionic-crystals). *Proceedings of the Royal Society-Mathematical and Physical Sciences* **1995**, 450, (1940), 501-512.

175. Garn, P. D., Kinetics of decomposition of the solid-state - is there really a dichotomy. *Thermochimica Acta* **1988**, 135, 71-77.

176. Niksa, S., Predicting the rapid devolatilization of diverse forms of biomass with bio-FLASHCHAIN. *Proceedings of the Combustion Institute* **2000**, 28, 2727-2733.

177. Solomon, P. R.; Hamblen, D. G.; Carangelo, R. M.; Serio, M. A.; Deshpande, G. V., General model of coal devolatilization. *Energy & Fuels* **1988**, 2, (4), 405-422.

178. Solomon, P. R., Advanced fuel-devolatilization model FG-DVC. In *ACS Division of Fuel Chemistry Preprints*, 1997; Vol. 35:2, pp 479-488.
179. Shafizadeh, F.; Chin, P. P. S., Thermal Deterioration of Wood. In *Abstracts of Papers of the American Chemical Society*, 1976; Vol. 43, pp 57-81.
180. Broido, A., Thermal Uses and Properties of Carbohydrates and Lignins. In *Thermal Uses and Properties of Carbohydrates and Lignins*, Shafizadeh, F.; Sarkanen, K.; Tillman, D. A., Eds. Academic: New York: 1976; pp 19-36.
181. Miller, R. S.; Bellan, J., A generalized biomass pyrolysis model based on superimposed cellulose, hemicellulose and lignin kinetics. *Combustion Science and Technology* **1997**, 126, (1-6), 97-137.
182. DiBlasi, C., Heat, momentum and mass transport through a shrinking biomass particle exposed to thermal radiation. *Chemical Engineering Science* **1996**, 51, (7), 1121-1132.
183. Corbetta, M.; Pierucci, S.; Ranzi, E.; Bennadji, H.; Fisher, E., Multistep kinetic model of biomass pyrolysis. In *Proceedings from the XXXVI Meeting of the Italian Section of the Combustion Institute*, 2013; pp 1-6.
184. Ranzi, E.; Corbetta, M.; Manenti, F.; Pierucci, S., Kinetic modeling of the thermal degradation and combustion of biomass. *Chemical Engineering Science* **2014**, 110, 2-12.
185. Ranzi, E.; Cuoci, A.; Faravelli, T.; Frassoldati, A.; Migliavacca, G.; Pierucci, S.; Sommariva, S., Chemical Kinetics of Biomass Pyrolysis. *Energy & Fuels* **2008**, 22, (6), 4292-4300.

186. Blondeau, J.; Jeanmart, H., Biomass pyrolysis at high temperatures: Prediction of gaseous species yields from an anisotropic particle. *Biomass & Bioenergy* **2012**, 41, 107-121.
187. Gomez, C. J.; Varhegyi, G.; Puigjaner, L., Slow pyrolysis of woody residues and an herbaceous biomass crop: A kinetic study. *Industrial & Engineering Chemistry Research* **2005**, 44, (17), 6650-6660.
188. Hu, M.; Chen, Z. H.; Wang, S. K.; Guo, D. B.; Ma, C. F.; Zhou, Y.; Chen, J.; Laghari, M.; Fazal, S.; Xiao, B.; Zhang, B. P.; Ma, S., Thermogravimetric kinetics of lignocellulosic biomass slow pyrolysis using distributed activation energy model, Fraser-Suzuki deconvolution, and iso-conversional method. *Energy Conversion and Management* **2016**, 118, 1-11.
189. Boutin, O.; Ferrer, M.; Lede, J., Flash pyrolysis of cellulose pellets submitted to a concentrated radiation: experiments and modelling. *Chemical Engineering Science* **2002**, 57, (1), 15-25.
190. Boutin, O.; Ferrer, M.; Lede, J., Radiant flash pyrolysis of cellulose - Evidence for the formation of short life time intermediate liquid species. *Journal of Analytical and Applied Pyrolysis* **1998**, 47, (1), 13-31.
191. Lede, J.; Blanchard, F.; Boutin, O., Radiant flash pyrolysis of cellulose pellets: products and mechanisms involved in transient and steady state conditions. *Fuel* **2002**, 81, (10), 1269-1279.
192. Liu, D. W.; Yu, Y.; Wu, H. W., Evolution of Water-Soluble and Water-Insoluble Portions in the Solid Products from Fast Pyrolysis of Amorphous Cellulose. *Industrial & Engineering Chemistry Research* **2013**, 52, (36), 12785-12793.

193. Gong, X.; Yu, Y.; Gao, X. P.; Qiao, Y.; Xu, M. H.; Wu, H. W., Formation of Anhydro-sugars in the Primary Volatiles and Solid Residues from Cellulose Fast Pyrolysis in a Wire-Mesh Reactor. *Energy & Fuels* **2014**, 28, (8), 5204-5211.
194. Pitt, G. J., The kinetics of the evolution of volatile products from coal. *Fuel* **1962**, 41, (3), 267-274.
195. Sonobe, T.; Worasuwanarak, N., Kinetic analyses of biomass pyrolysis using the distributed activation energy model. *Fuel* **2008**, 87, (3), 414-421.
196. Cai, J. M.; Liu, R. H., New distributed activation energy model: Numerical solution and application to pyrolysis kinetics of some types of biomass. *Bioresource Technology* **2008**, 99, (8), 2795-2799.
197. de Caprariis, B.; Santarelli, M.; Scarsella, M.; Herce, C.; Verdone, N.; De Filippis, P., Kinetic analysis of biomass pyrolysis using a double distributed activation energy model. *Journal of Thermal Analysis and Calorimetry* **2015**, 121, (3), 1403-1410.
198. Li, C. S.; Suzuki, K., Kinetic analyses of biomass tar pyrolysis using the distributed activation energy model by TG/DTA technique. *Journal of Thermal Analysis and Calorimetry* **2009**, 98, (1), 261-266.
199. Cai, J. M.; Wu, W. X.; Liu, R. H., An overview of distributed activation energy model and its application in the pyrolysis of lignocellulosic biomass. *Renewable & Sustainable Energy Reviews* **2014**, 36, 236-246.
200. Alves, S. S.; Figueiredo, J. L., Kinetics of cellulose pyrolysis modeled by 3 consecutive first-order reactions. *Journal of Analytical and Applied Pyrolysis* **1989**, 17, (1), 37-46.

201. Burra, K. R. G.; Gupta, A. K., Modeling of biomass pyrolysis kinetics using sequential multi-step reaction model. *Fuel* **2019**, 237, 1057-1067.

202. Vinu, R.; Broadbelt, L. J., A mechanistic model of fast pyrolysis of glucose-based carbohydrates to predict bio-oil composition. *Energy & Environmental Science* **2012**, 5, (12), 9808-9826.

203. Zhou, X. W.; Li, W. J.; Mabon, R.; Broadbelt, L. J., A mechanistic model of fast pyrolysis of hemicellulose. *Energy & Environmental Science* **2018**, 11, (5), 1240-1260.

204. Gubaev, K.; Podryabinkin, E. V.; Hart, G. L. W.; Shapeev, A. V., Accelerating high-throughput searches for new alloys with active learning of interatomic potentials. *Computational Materials Science* **2019**, 156, 148-156.

205. Haghighatlari, M.; Hachmann, J., Advances of machine learning in molecular modeling and simulation. *Current Opinion in Chemical Engineering* **2019**, (23), 51-57.

206. Alberi, K.; Nardelli, M. B.; Zakutayev, A.; Mitas, L.; Curtarolo, S.; Jain, A.; Fornari, M.; Marzari, N.; Takeuchi, I.; Green, M. L.; Kanatzidis, M.; Toney, M. F.; Butenko, S.; Meredig, B.; Lany, S.; Kattner, U.; Davydov, A.; Toberer, E. S.; Stevanovic, V.; Walsh, A.; Park, N. G.; Aspuru-Guzik, A.; Tabor, D. P.; Nelson, J.; Murphy, J.; Setlur, A.; Gregoire, J.; Li, H.; Xiao, R. J.; Ludwig, A.; Martin, L. W.; Rappe, A. M.; Wei, S. H.; Perkins, J., The 2019 materials by design roadmap. *Journal of Physics D-Applied Physics* **2019**, 52, (1).

207. Ulissi, Z. W.; Tang, M. T.; Xiao, J. P.; Liu, X. Y.; Torelli, D. A.; Karamad, M.; Cummins, K.; Hahn, C.; Lewis, N. S.; Jaramillo, T. F.; Chan, K. R.; Norskov, J. K., Machine-Learning

Methods Enable Exhaustive Searches for Active Bimetallic Facets and Reveal Active Site Motifs for CO₂ Reduction. *ACS Catalysis* **2017**, 7, (10), 6600-6608.

208. Ali, J. M.; Hussain, M. A.; Tade, M. O.; Zhang, J., Artificial Intelligence techniques applied as estimator in chemical process systems - A literature survey. *Expert Systems with Applications* **2015**, 42, (14), 5915-5931.

209. Conesa, J. A.; Caballero, J. A.; Reyes-Labarta, J. A., Artificial neural network for modelling thermal decompositions. *Journal of Analytical and Applied Pyrolysis* **2004**, 71, (1), 343-352.

210. Ghadrhan, M.; Mehdizadeh, H.; Boozarjomehry, R. B.; Darian, J. T., On the Introduction of a Qualitative Variable to the Neural Network for Reactor Modeling: Feed Type. *Industrial & Engineering Chemistry Research* **2009**, 48, (8), 3820-3824.

211. Zakrzewska, B.; Jaworski, Z., An Empirical Model of a Multiphase Reactor Based on Artificial Neural Network. In *Icheap-9: 9th International Conference on Chemical and Process Engineering, Pts 1-3*, Pierucci, S., Ed. 2009; Vol. 17, pp 1239-1244.

212. Sharma, R.; Singh, K.; Singhal, D.; Ghosh, R., Neural network applications for detecting process faults in packed towers. *Chemical Engineering and Processing* **2004**, 43, (7), 841-847.

213. Hough, B. R.; Beck, D. A. C.; Schwartz, D. T.; Pfaendtner, J., Application of machine learning to pyrolysis reaction networks: Reducing model solution time to enable process optimization. *Computers & Chemical Engineering* **2017**, 104, 56-63.

214. Hough, B. R.; Schwartz, D. T.; Pfaendtner, J., Detailed Kinetic Modeling of Lignin Pyrolysis for Process Optimization. *Industrial & Engineering Chemistry Research* **2016**, 55, (34), 9147-9153.

215. Furutani, Y.; Kudo, S.; Hayashi, J.; Norinaga, K., Predicting molecular composition of primary product derived from fast pyrolysis of lignin with semi-detailed kinetic model. *Fuel* **2018**, 212, 515-522.

216. Hua, F.; Fang, Z.; Qiu, T., Application of convolutional neural networks to large-scale naphtha pyrolysis kinetic modeling. *Chinese Journal of Chemical Engineering* **2018**, 26, (12), 2562-2572.

217. Lerkkasemsan, N.; Achenie, L. E. K., Pyrolysis of biomass - fuzzy modeling. *Renewable Energy* **2014**, 66, 747-758.

218. Nieto, P. J. G.; Garcia-Gonzalo, E.; Lasheras, F. S.; Paredes-Sanchez, J. P.; Fernandez, P. R., Forecast of the higher heating value in biomass torrefaction by means of machine learning techniques. *Journal of Computational and Applied Mathematics* **2019**, 357, 284-301.

219. Jiang, W.; Xing, X. J.; Li, S.; Zhang, X. W.; Wang, W. Q., Synthesis, characterization and machine learning based performance prediction of straw activated carbon. *Journal of Cleaner Production* **2019**, 212, 1210-1223.

220. Zhu, W.; Ma, Y.; Benton, M. G.; Romagnoli, J. A.; Zhan, Y., Deep learning for pyrolysis reactor monitoring: From thermal imaging toward smart monitoring system. *Aiche J.* **2019**, 65, (2), 582-591.

221. Francisco-Fernandez, M.; Tarrio-Saavedra, J.; Naya, S.; Lopez-Beceiro, J.; Artiaga, R., Classification of wood using differential thermogravimetric analysis. *Journal of Thermal Analysis and Calorimetry* **2015**, 120, (1), 541-551.

222. Nabavi, R.; Salari, D.; Niaei, A.; Vakil-Baghmisheh, M. T., A Neural Network Approach for Prediction of Main Product Yields in Methanol to Olefins Process. *International Journal of Chemical Reactor Engineering* **2009**, 7.

223. Stamenkovic, O. S.; Rajkovic, K.; Velickovic, A. V.; Mille, P. S.; Veljkovic, V. B., Optimization of base-catalyzed ethanolysis of sunflower oil by regression and artificial neural network models. *Fuel Processing Technology* **2013**, 114, 101-108.

224. Cheng, M. Y.; Prayogo, D.; Ju, Y. H.; Wu, Y. W.; Sutanto, S., Optimizing mixture properties of biodiesel production using genetic algorithm-based evolutionary support vector machine. *International Journal of Green Energy* **2016**, 13, (15), 1599-1607.

225. Saldana, D. A.; Starck, L.; Mougin, P.; Rousseau, B.; Creton, B., Prediction of Flash Points for Fuel Mixtures Using Machine Learning and a Novel Equation. *Energy & Fuels* **2013**, 27, (7), 3811-3820.

226. Arabloo, M.; Bahadori, A.; Ghiasi, M. M.; Lee, M.; Abbas, A.; Zendehboudi, S., A novel modeling approach to optimize oxygen-steam ratios in coal gasification process. *Fuel* **2015**, 153, 1-5.

227. Tan, P.; Xia, J.; Zhang, C.; Fang, Q. Y.; Chen, G., Modeling and reduction of NOX emissions for a 700 MW coal-fired boiler with the advanced machine learning method. *Energy* **2016**, 94, 672-679.

228. Zhang, Y. N.; Brown, T. R.; Hu, G. P.; Brown, R. C., Techno-economic analysis of two bio-oil upgrading pathways. *Chemical Engineering Journal* **2013**, 225, 895-904.

229. Yang, Z.; Kumar, A.; Huhnke, R. L., Review of recent developments to improve storage and transportation stability of bio-oil. *Renewable & Sustainable Energy Reviews* **2015**, 50, 859-870.

230. Sahebjamnia, N.; Tavakkoli-Moghaddam, R.; Ghorbani, N., Designing a fuzzy Q-learning multi-agent quality control system for a continuous chemical production line - A case study. *Computers & Industrial Engineering* **2016**, 93, 215-226.

231. Matthews, A. G. D.; van der Wilk, M.; Nickson, T.; Fujii, K.; Boukouvalas, A.; Leon-Villagra, P.; Ghahramani, Z.; Hensman, J., GPflow: A Gaussian Process Library using TensorFlow. *Journal of Machine Learning Research* **2017**, 18, 1-6.

232. Wongsuphasawat, K.; Smilkov, D.; Wexler, J.; Wilson, J.; Mane, D.; Fritz, D.; Krishnan, D.; Viegas, F. B.; Wattenberg, M., Visualizing Dataflow Graphs of Deep Learning Models in TensorFlow. *IEEE Transactions on Visualization and Computer Graphics* **2018**, 24, (1), 1-12.